Measurement of the neutrino velocity with the OPERA detector in the CNGS beam[*]

T. Adam[a], N. Agafonova[b], A. Aleksandrov[c,1], O. Altinok[d], P. Alvarez Sanchez[e], A. Anokhina[f], S. Aoki[g], A. Ariga[h], T. Ariga[h], D. Autiero[i†], A. Badertscher[j], A. Ben Dhahbi[h], A. Bertolin[k], C. Bozza[l], T. Brugière[i], R. Brugnera[m,k], F. Brunet[n], G. Brunetti[o,i,2], S. Buontempo[c], B. Carlus[i], F. Cavanna[q], A. Cazes[i], L. Chaussard[i], M. Chernyavsky[r], V. Chiarella[s], A. Chukanov[t], G. Colosimo[u], M. Crespi[u], N. D'Ambrosio[v], G. De Lellis[w,c], M. De Serio[x], Y. Déclais[i], P. del Amo Sanchez[n], F. Di Capua[c], A. Di Crescenzo[w,c], D. Di Ferdinando[p], N. Di Marco[v], S. Dmitrievsky[t], M. Dracos[a], D. Duchesneau[n], S. Dusini[k], J. Ebert[y], I. Efthymiopoulos[e], O. Egorov[z], A. Ereditato[h], L.S. Esposito[j], J. Favier[n], T. Ferber[y], R.A. Fini[x], T. Fukuda[aa], A. Garfagnini[m,k], G. Giacomelli[o,p], M. Giorgini[o,p,3], M. Giovannozzi[e], C. Girerd[i], J. Goldberg[ab], C. Göllnitz[y], D. Golubkov[z], L. Goncharova[r], Y. Gornushkin[t], G. Grella[l], F. Grianti[s,ac], E. Gschwendtner[e], C. Guerin[i], A.M. Guler[d], C. Gustavino[ad], C. Hagner[y], K. Hamada[ae], T. Hara[g], M. Hierholzer[y], A. Hollnagel[y], M. Ieva[x], H. Ishida[aa], K. Ishiguro[ae], K. Jakovcic[af], C. Jollet[a], M. Jones[e], F. Juget[h], M. Kamiscioglu[d], J. Kawada[h], S.H. Kim[ag,4], M. Kimura[aa], E. Kiritsis[ah], N. Kitagawa[ae], B. Klicek[af], J. Knuesel[h], K. Kodama[ai], M. Komatsu[ae], U. Kose[k], I. Kreslo[h], C. Lazzaro[j], J. Lenkeit[y], A. Ljubicic[af], A. Longhin[s], A. Malgin[b], G. Mandrioli[p], J. Marteau[i], T. Matsuo[aa], N. Mauri[s], A. Mazzoni[u], E. Medinaceli[m,k], F. Meisel[h], A. Meregaglia[a], P. Migliozzi[c], S. Mikado[aa], D. Missiaen[e], K. Morishima[ae], U. Moser[h], M.T. Muciaccia[aj,x], N. Naganawa[ae], T. Naka[ae], M. Nakamura[ae], T. Nakano[ae], Y. Nakatsuka[ae], V. Nikitina[f], F. Nitti[ak], S. Ogawa[aa], N. Okateva[r], A. Olchevsky[t], O. Palamara[v], A. Paoloni[s], B.D. Park[ag,5], I.G. Park[ag], A. Pastore[aj,x], L. Patrizii[p], E. Pennacchio[i], H. Pessard[n], C. Pistillo[h], N. Polukhina[r], M. Pozzato[o,p], K. Pretzl[h], F. Pupilli[v], R. Rescigno[l], F. Riguzzi[al], T. Roganova[f], H. Rokujo[g], G. Rosa[am,ad], I. Rostovtseva[z], A. Rubbia[j], A. Russo[c], O. Sato[ae], Y. Sato[an], J. Schuler[a], L. Scotto Lavina[h,6], J. Serrano[e], A. Sheshukov[t], H. Shibuya[aa], G. Shoziyoev[f], S. Simone[aj,x], M. Sioli[o,p], C. Sirignano[v], G. Sirri[p], J.S. Song[ag], M. Spinetti[s], L. Stanco[k], N. Starkov[r], S. Stellacci[l], M. Stipcevic[af], T. Strauss[h], S. Takahashi[g], M. Tenti[o,p,i], F. Terranova[s,ao], I. Tezuka[an], V. Tioukov[c], P. Tolun[d], N.T. Tran[i], S. Tufanli[h], P. Vilain[ap], M. Vladimirov[r], L. Votano[s], J.-L. Vuilleumier[h], G. Wilquet[ap], B. Wonsak[y], J. Wurtz[a], C.S. Yoon[ag], J. Yoshida[ae], Y. Zaitsev[z], S. Zemskova[t], A. Zghiche[n]

[a] IPHC, Université de Strasbourg, CNRS/IN2P3, F-67037 Strasbourg, France
[b] INR-Institute for Nuclear Research of the Russian Academy of Sciences, RUS-327312 Moscow, Russia
[c] INFN Sezione di Napoli, I-80125 Napoli, Italy
[d] METU-Middle East Technical University, TR-06532 Ankara, Turkey
[e] European Organization for Nuclear Research (CERN), Geneva, Switzerland
[f] (MSU SINP) Lomonosov Moscow State University Skobeltsyn Institute of Nuclear Physics, RUS-119992 Moscow, Russia
[g] Kobe University, J-657-8501 Kobe, Japan
[h] Albert Einstein Center for Fundamental Physics, Laboratory for High Energy Physics (LHEP), University of Bern, CH-3012 Bern, Switzerland
[i] IPNL, Université Claude Bernard Lyon I, CNRS/IN2P3, F-69622 Villeurbanne, France
[j] ETH Zurich, Institute for Particle Physics, CH-8093 Zurich, Switzerland

[k] INFN Sezione di Padova, I-35131 Padova, Italy

[l] Dipartimento di Fisica dell'Università di Salerno and INFN "Gruppo Collegato di Salerno", I-84084 Fisciano, Salerno, Italy

[m] Dipartimento di Fisica dell'Università di Padova, 35131 I-Padova, Italy

[n] LAPP, Université de Savoie, CNRS/IN2P3, F-74941 Annecy-le-Vieux, France

[o] Dipartimento di Fisica dell'Università di Bologna, I-40127 Bologna, Italy

[p] INFN Sezione di Bologna, I-40127 Bologna, Italy

[q] Dipartimento di Fisica dell'Università dell'Aquila and INFN "Gruppo Collegato de L'Aquila", I-67100 L'Aquila, Italy

[r] LPI-Lebedev Physical Institute of the Russian Academy of Science, RUS-119991 Moscow, Russia

[s] INFN - Laboratori Nazionali di Frascati, I-00044 Frascati (Roma), Italy

[t] JINR-Joint Institute for Nuclear Research, RUS-141980 Dubna, Russia

[u] Area di Geodesia e Geomatica, Dipartimento di Ingegneria Civile Edile e Ambientale dell'Università di Roma Sapienza, I-00185 Roma, Italy

[v] INFN - Laboratori Nazionali del Gran Sasso, I-67010 Assergi (L'Aquila), Italy

[w] Dipartimento di Scienze Fisiche dell'Università Federico II di Napoli, I-80125 Napoli, Italy

[x] INFN Sezione di Bari, I-70126 Bari, Italy

[y] Hamburg University, D-22761 Hamburg, Germany

[z] ITEP-Institute for Theoretical and Experimental Physics RUS-117259 Moscow, Russia

[aa] Toho University, J-274-8510 Funabashi, Japan

[ab] Department of Physics, Technion, IL-32000 Haifa, Israel

[ac] Università degli Studi di Urbino "Carlo Bo", I-61029 Urbino - Italy

[ad] INFN Sezione di Roma , I-00185 Roma, Italy

[ae] Nagoya University, J-464-8602 Nagoya, Japan

[af] IRB-Rudjer Boskovic Institute, HR-10002 Zagreb, Croatia

[ag] Gyeongsang National University, ROK-900 Gazwa-dong, Jinju 660-701, Korea

[ah] Crete Center for Theoretical Physics, Department of Physics, University of Crete, GR-71003 Heraklion, Greece

[ai] Aichi University of Education, J-448-8542 Kariya (Aichi-Ken), Japan

[aj] Dipartimento di Fisica dell'Università di Bari, I-70126 Bari, Italy

[ak] Theory Division APC, Université Paris 7, Bâtiment Condorcet, F-75205, Paris Cedex 13, France

[al] Istituto Nazionale di Geofisica e Vulcanologia, Sez. CNT, I-00143 Roma, Italy

[am] Dipartimento di Fisica dell'Università di Roma Sapienza, I-00185 Roma, Italy

[an] Utsunomiya University, J-321-8505 Utsunomiya, Japan

[ao] Dipartimento di Fisica dell' Università di Milano-Bicocca, I-20126 Milano, Italy

[ap] IIHE, Université Libre de Bruxelles, B-1050 Brussels, Belgium

[1] On leave of absence from LPI-Lebedev Physical Institute of the Russian Academy of Sciences, 119991 Moscow, Russia

[2] Now at Albert Einstein Center for Fundamental Physics, Laboratory for High Energy Physics (LHEP), University of Bern, CH-3012 Bern, Switzerland

[3] Now at INAF/IASF, Sezione di Milano, I-20133 Milano, Italy

[4] Now at Pusan National University, Geumjeong-Gu, Busan 609-735, Republic of Korea

[5] Now at Asan Medical Center, 388-1 Pungnap-2 Dong, Songpa-Gu, Seoul 138-736, Republic of Korea

[6] Now at SUBATECH, CNRS/IN2P3, F-44307 Nantes, France

Abstract

The OPERA neutrino experiment at the underground Gran Sasso Laboratory has measured the velocity of neutrinos from the CERN CNGS beam over a baseline of about 730 km with much higher accuracy than previous studies conducted with accelerator neutrinos. The measurement is based on high-statistics data taken by OPERA in the years 2009, 2010 and 2011. Dedicated upgrades of the CNGS timing system and of the OPERA detector, as well as a high precision geodesy campaign for the measurement of the neutrino baseline, allowed reaching comparable systematic and statistical accuracies. An early arrival time of CNGS muon neutrinos with respect to the one computed assuming the speed of light in vacuum of $(57.8 \pm 7.8 \text{ (stat.) } {}^{+8.3}_{-5.9} \text{ (sys.)})$ ns was measured. This anomaly corresponds to a relative difference of the muon neutrino velocity with respect to the speed of light $(v\text{-}c)/c = (2.37 \pm 0.32 \text{ (stat.)} {}^{+0.34}_{-0.24} \text{ (sys.)}) \times 10^{-5}$. The above result, obtained by comparing the time distributions of neutrino interactions and of protons hitting the CNGS target in 10.5 μs long extractions, was confirmed by a test performed using a beam with a short-bunch time-structure allowing to measure the neutrino time of flight at the single interaction level.

1. Introduction

The OPERA neutrino experiment [1] at the underground Gran Sasso Laboratory (LNGS) was designed to perform the first detection of neutrino oscillations in direct appearance mode in the $\nu_\mu \rightarrow \nu_\tau$ channel, the signature being the identification of the τ^- lepton created by its charged current (CC) interaction [2].

In addition to its main goal, the experiment is well suited to determine the neutrino velocity with high accuracy through the measurement of the time of flight and of the distance between the source of the CNGS neutrino beam at CERN (CERN Neutrino beam to Gran Sasso) [3] and the OPERA detector at LNGS. For CNGS neutrino energies, $<E_\nu> = 17$ GeV, the relative deviation from the speed of light c of the neutrino velocity due to its finite rest mass is expected to be smaller than 10^{-19}, even assuming the mass of the heaviest neutrino *eigenstate* to be as large as 2 eV [4]. Hence, a larger deviation of the neutrino velocity from c would be a striking result pointing to new physics in the neutrino sector. So far, no established deviation has been observed by any experiment.

In the past, a high energy ($E_\nu > 30$ GeV) and short baseline experiment has been able to test deviations down to $|v\text{-}c|/c < 4 \times 10^{-5}$ [5]. With a baseline analogous to that of OPERA but at lower neutrino energies (E_ν peaking at ~3 GeV with a tail extending above 100 GeV), the MINOS experiment reported a measurement of $(v\text{-}c)/c = (5.1 \pm 2.9) \times 10^{-5}$ [6]. At much lower energy, in the 10 MeV range, a stringent limit of $|v\text{-}c|/c < 2 \times 10^{-9}$ was set by the observation of (anti) neutrinos emitted by the SN1987A supernova [7].

In this paper we report on the precision determination of the neutrino velocity, defined as the ratio of the precisely measured distance from CERN to OPERA to the time of flight of neutrinos travelling through the Earth's crust. We used the high-statistics data taken by OPERA in the years 2009, 2010 and 2011. Dedicated upgrades of the timing systems for the time tagging and synchronisation of the CNGS beam at CERN and of the OPERA detector at LNGS resulted in a reduction of the systematic uncertainties down to the level of the statistical error. The

measurement also relies on a high-accuracy geodesy campaign that allowed measuring the 730 km CNGS baseline with a precision of 20 cm.

With the objective of performing further checks of the result reported here, very recently we have been able to conduct a measurement of the neutrino time of flight at the single interaction level by using a beam test with a short-bunch time-structure.

2. The OPERA detector and the CNGS neutrino beam

The OPERA neutrino detector at LNGS is composed of two identical Super Modules, each consisting of an instrumented target section with a mass of about 625 tons followed by a magnetic muon spectrometer. Each section is a succession of walls filled with emulsion film/lead units interleaved with pairs of 6.7×6.7 m^2 planes of 256 horizontal and vertical scintillator strips composing the Target Tracker (TT). The TT allows the location of neutrino interactions in the target. This detector is also used to measure the arrival time of neutrinos. The scintillating strips are read out on both sides through WLS Kuraray Y11 fibres coupled to 64-channel Hamamatsu H7546 photomultipliers [8]. Extensive information on the OPERA experiment is given in [1] and in particular for the TT in [9].
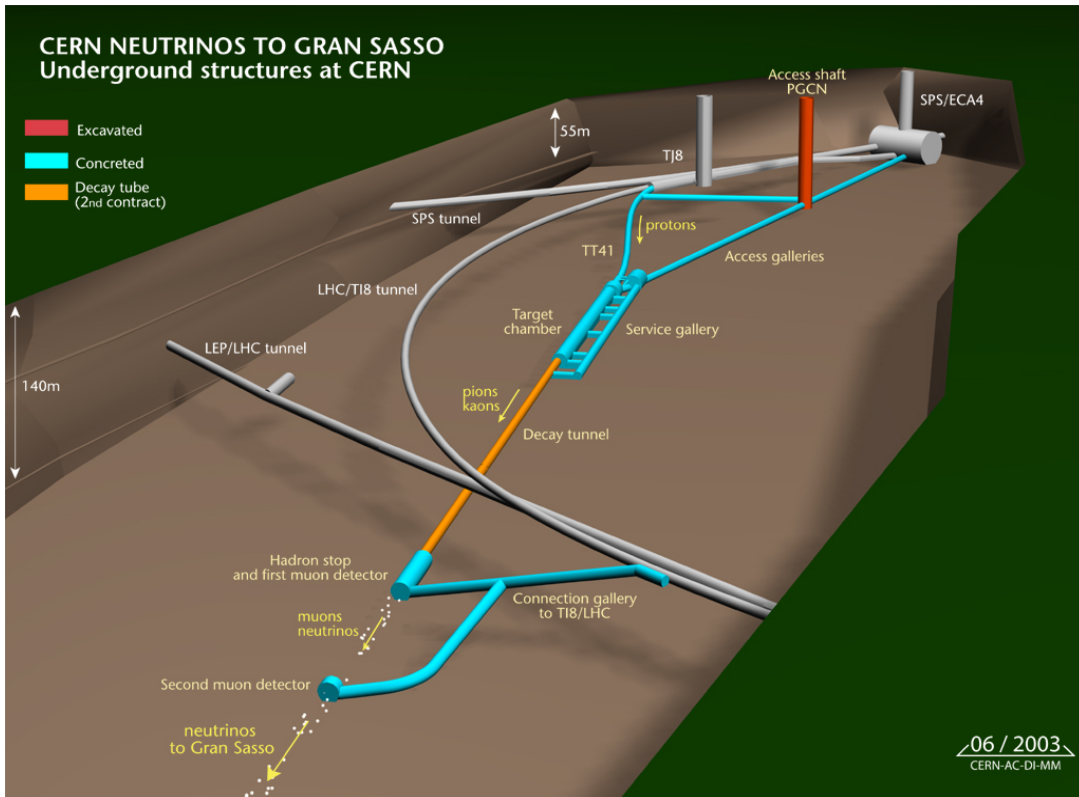

Fig. 1: Artistic view of the SPS/CNGS layout.

The CNGS beam is produced by accelerating protons to 400 GeV/c with the CERN Super Proton Synchrotron (SPS). These protons are ejected with a kicker magnet towards a 2 m long

graphite neutrino production target in two extractions, each lasting 10.5 μs and separated by 50 ms. Each CNGS cycle in the SPS is 6 s long. Secondary charged mesons are focused by a magnetic horn and reflector, each followed by a helium bag to minimise the interaction probability of the mesons. These decay in flight into neutrinos in a 1000 m long vacuum tunnel. The SPS/CNGS layout is shown in Fig. 1. The different components of the CNGS beam are shown in Fig. 2.

The distance between the neutrino target and the OPERA detector is about 730 km. The CNGS beam is an almost pure ν_μ beam with an average energy of 17 GeV, optimised for $\nu_\mu \to \nu_\tau$ appearance oscillation studies. In terms of interactions in the detector, the $\overline{\nu}_\mu$ contamination is 2.1%, while ν_e and $\overline{\nu}_e$ contaminations are together smaller than 1%. The FWHM of the neutrino beam at the OPERA location is 2.8 km.
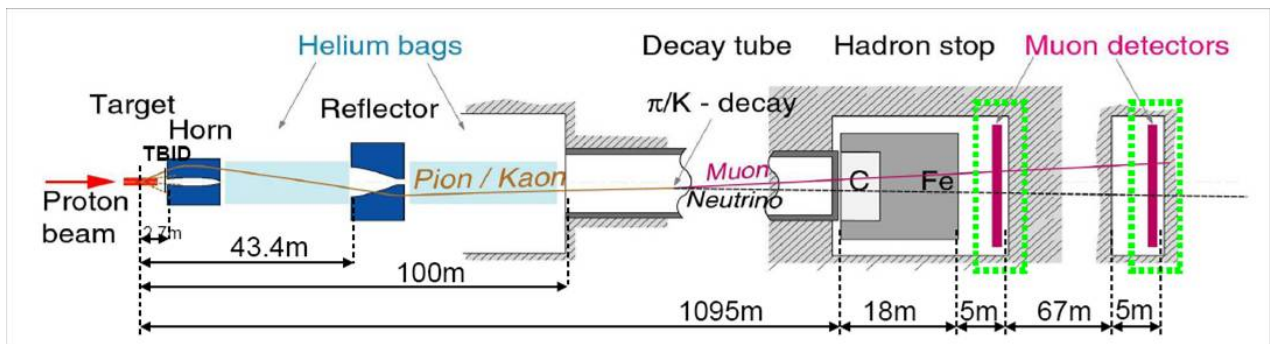

Fig.2: Layout of the CNGS beam line.

The kicker magnet trigger-signal for the proton extraction from the SPS is UTC (Coordinated Universal Time) time-stamped with a Symmetricom Xli GPS receiver [10]. The schematic of the SPS/CNGS timing system is shown in Fig. 3. The determination of the delays shown in Fig. 3 is described in section 6.

The proton beam time-structure is accurately measured by a fast Beam Current Transformer (BCT) detector [11] (BFCTI400344) located (743.391 ± 0.002) m upstream of the centre of the graphite target and read out by a 1 GS/s Wave Form Digitiser (WFD) Acqiris DP110 with a 250 MHz bandwidth [12]. The BCT consists of toroidal transformers coaxial to the proton beam providing a signal proportional to the beam current transiting through it, with a 400 MHz bandwidth. The linearity of the device is better than 1% and it is operated far from the saturation limit. The start of the digitisation window of the WFD is triggered by the kicker magnet signal. The waveforms recorded for each extraction by the WFD are stamped with the UTC and stored in the CNGS database.

The intensity of the proton beam in the SPS features a five-step structure reflecting the five-turn (2.1 μs per turn) Continuous Transfer (CT) extraction mode from the CERN Proton Synchrotron (PS), as seen in the left part of Fig. 4. The fine structure due to the 200 MHz SPS radiofrequency is superimposed, which is actually resolved by the BCT measurement (Fig. 4, right).
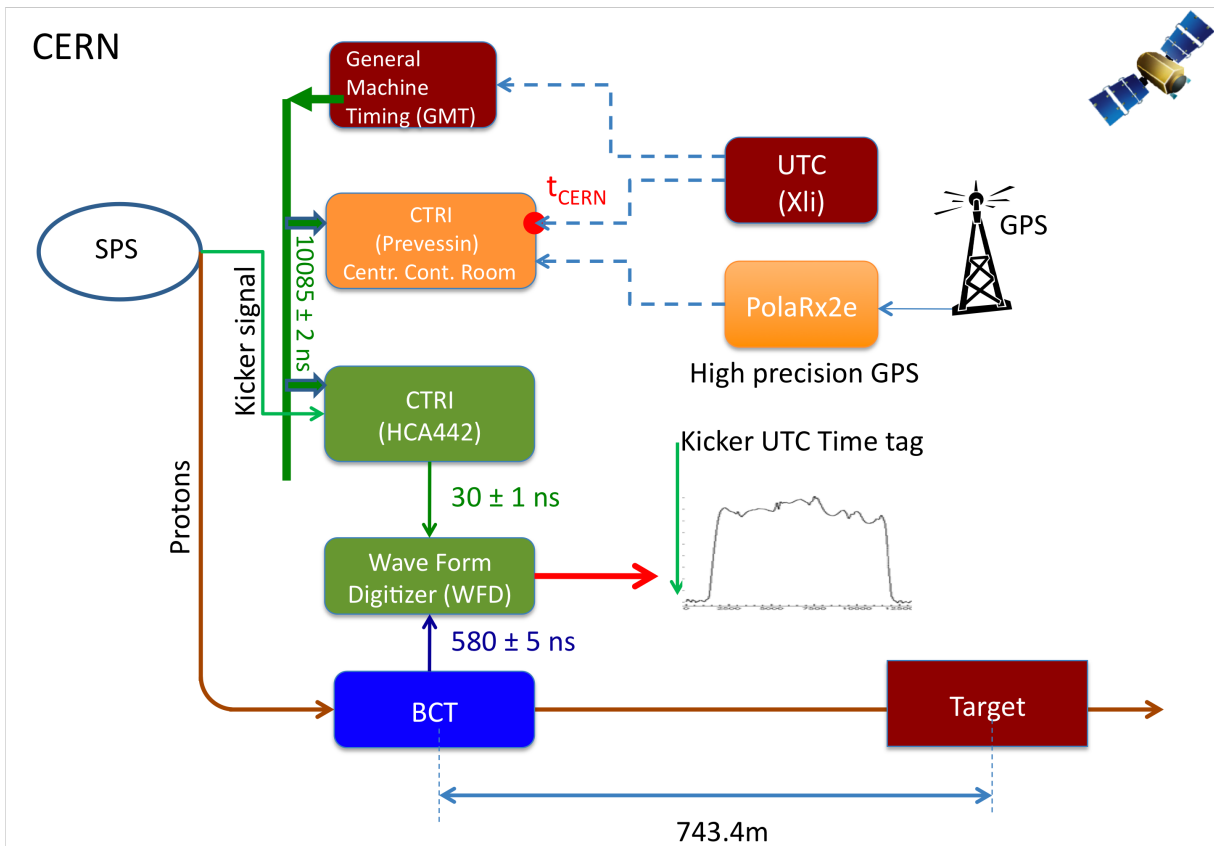
Fig. 3: Schematic of the CERN SPS/CNGS timing system. Green boxes indicate detector time-response. Orange boxes refer to elements of the CNGS-OPERA synchronisation system. Details on the various elements are given in section 6.
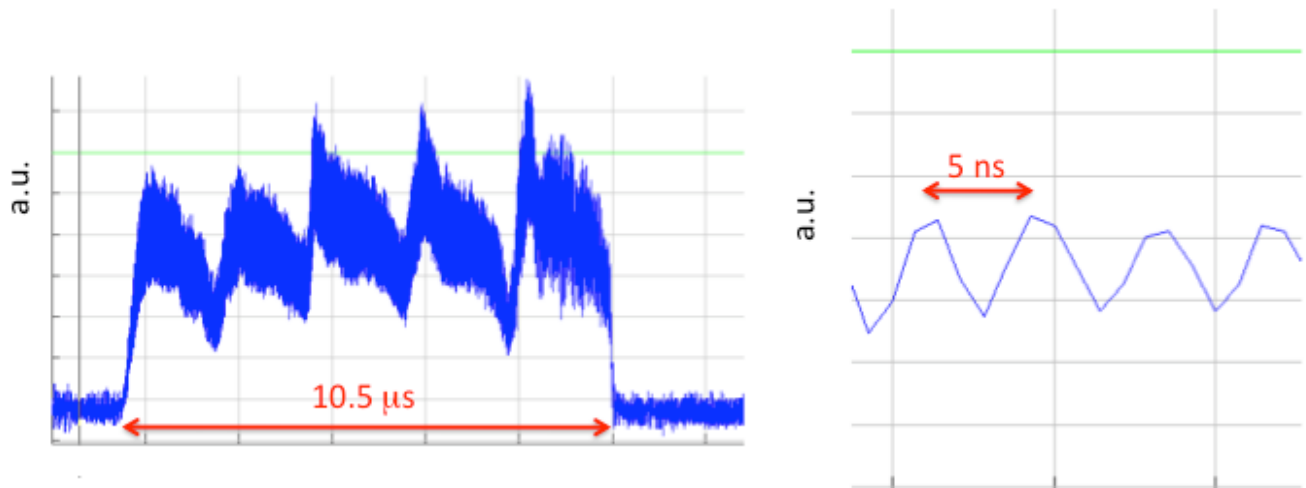
Fig. 4: Example of a specially selected proton extraction waveform measured with the BCT detector BFCTI400344, to show the five-peak structure reflecting the proton losses in the PS Continuous Transfer extraction mechanism. This structure is more pronounced than for the majority of the waveforms. A blow-up of the waveform (right plot) shows that the 200 MHz SPS radiofrequency is resolved.

6

3. Principle of the neutrino time of flight measurement

A schematic description of the principle of the time of flight measurement is shown in Fig. 5. The time of flight of CNGS neutrinos (TOF_ν) cannot be precisely measured at the single interaction level since any proton in the 10.5 μs extraction time may produce the neutrino detected by OPERA. However, by measuring the time distributions of protons for each extraction for which neutrino interactions are observed in the detector, and summing them together, after proper normalisation one obtains the probability density function (PDF) of the time of emission of the neutrinos within the duration of extraction. Each proton waveform is UTC time-stamped as well as the events detected by OPERA. The two time-stamps are related by TOF_c, the expected time of flight assuming the speed of light [13]. It is worth stressing that this measurement does not rely on the difference between a start and a stop signal but on the comparison of two event time distributions.
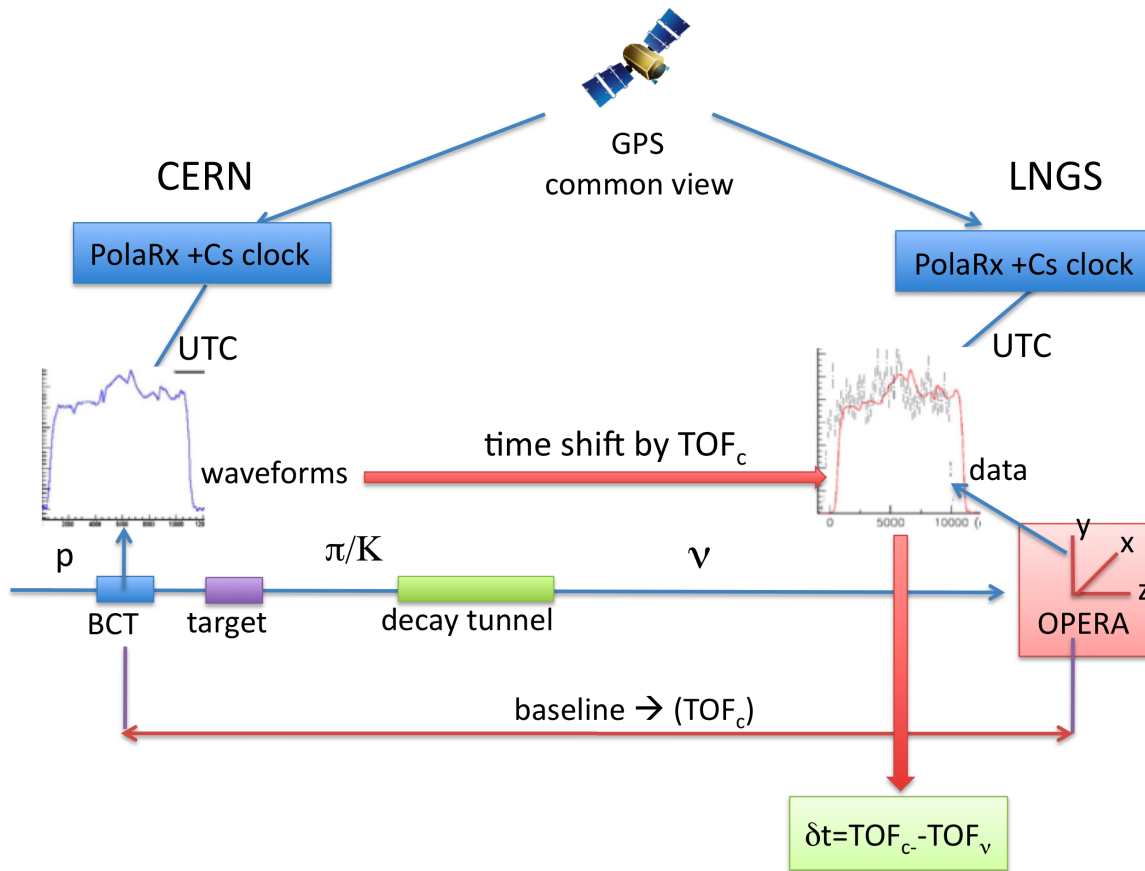
Fig. 5: Schematic of the time of flight measurement.

The PDF distribution can then be compared with the time distribution of the interactions detected in OPERA, in order to measure TOF_ν. The deviation $\delta t = TOF_c - TOF_\nu$ is obtained by a maximum likelihood analysis of the time tags of the OPERA events with respect to the PDF, as a function of δt. The individual measurement of the waveforms reflecting the time structure of the extraction reduces systematic effects related to time variations of the beam compared to the case

where the beam time structure is measured on average, *e.g.* by a near neutrino detector without using proton waveforms.

The total statistics used for the analysis reported in this paper is of 15223 events detected in OPERA, corresponding to about 10^{20} protons on target collected during the 2009, 2010 and 2011 CNGS runs. This allowed estimating δt with a small statistical uncertainty, presently comparable to the total systematic uncertainty.

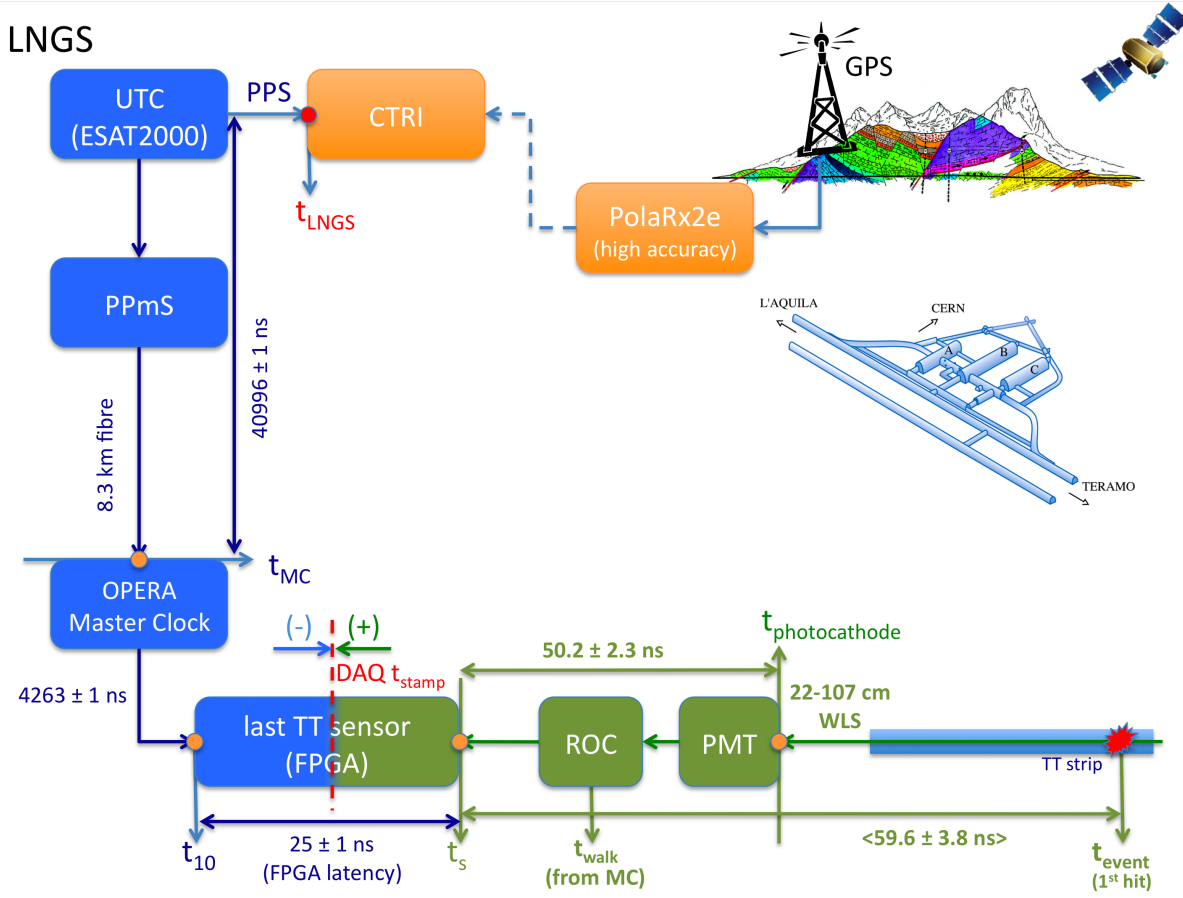Fig. 6: Schematic of the OPERA timing system at LNGS. Blue delays include elements of the time-stamp distribution; increasing delays decrease the value of δt. Green delays indicate detector time-response; increasing delays increase the value of δt. Orange boxes refer to elements of the CNGS-OPERA synchronisation system.

The point where the parent meson produces a neutrino in the decay tunnel is unknown. However, this introduces a negligible inaccuracy in the neutrino time of flight measurement, because the produced mesons are ultra-relativistic. This affects TOF_ν by a correction of the order of $d/2c\gamma^2$, with d being the meson decay length, on average ~ 450 m from the target, and γ its Lorentz factor, on average as large as 190. By a full FLUKA-based simulation of the CNGS beam [14] it was shown that the time difference computed assuming a particle moving at the speed of light from the target down to LNGS, with respect to the value derived by taking into account the speed of the relativistic parent meson down to its decay point is less than 0.02 ns. Similar arguments apply to muons produced in muon neutrino CC interactions occurring in the rock in front of the OPERA detector and seen in the apparatus (external events). With a full GEANT simulation of external events it is shown that ignoring the position of the interaction

point in the rock introduces a bias smaller than 2 ns with respect to those events occurring in the target (internal events), provided that external interactions are selected by requiring identified muons in OPERA. More details on the muon identification procedure are given in [15].

A key feature of the neutrino velocity measurement is the accuracy of the relative time tagging at CERN and at the OPERA detector. The standard GPS receivers formerly installed at CERN and LNGS would feature an insufficient ~100 ns accuracy for the TOF_v measurement. Thus, in 2008, two identical systems, composed of a GPS receiver for time-transfer applications Septentrio PolaRx2e [16] operating in "common-view" mode [17] and a Cs atomic clock Symmetricom Cs4000 [18], were installed at CERN and LNGS (see Figs. 3, 5 and 6).

The Cs4000 oscillator provides the reference frequency to the PolaRx2e receiver, which is able to time-tag its "One Pulse Per Second" output (1PPS) with respect to the individual GPS satellite observations. The latter are processed offline by using the CGGTTS format [19]. The two systems feature a technology routinely used for high-accuracy time-transfer applications by national time and frequency metrology laboratories around the world, in order to compare atomic clocks [20]. These international time comparisons are the basis of the UTC as defined by the Bureau International des Poids et Mesures (BIPM). The two systems were calibrated in 2008 by the Federal Swiss Metrology Institute METAS (Bundesamt für Metrologie) [21] and established a permanent time link at the 2 ns level between two reference points (t_{CERN} and t_{LNGS}) of the timing chains at CERN and OPERA. This time link was independently verified in 2011 by the Federal German Metrology Institute PTB (Physikalisch-Technische Bundesanstalt) [22] by taking data at CERN and LNGS with a portable time-transfer device commonly employed for relative time link calibrations [23]. The difference between the time base of the CERN and OPERA PolaRx2e receivers was measured to be (2.3 ± 0.9) ns [22]. This correction was taken into account in the application of the time link.

All the other elements of the timing distribution chains of CERN and OPERA were accurately calibrated by using different techniques, further described in the following, in order to reach a comparable level of accuracy.

4. Measurement of the neutrino baseline

The other fundamental ingredient for the neutrino velocity measurement is the knowledge of the distance between the point where the proton time-structure is measured at CERN and the origin of the underground OPERA detector reference frame at LNGS. The relative positions of the elements of the CNGS beam line are known with millimetre accuracy. When these coordinates are transformed into the global geodesy reference frame ETRF2000 [24] by relating them to external GPS benchmarks, they are known within 2 cm accuracy. This frame has a scale error at the level of 10^{-9} [25].

The analysis of the GPS benchmark positions was first done by extrapolating measurements taken at different periods via geodynamical models [26], and then by comparing simultaneous measurements taken in the same reference frame. The two methods yielded the same result within 2 cm [25]. The travel path of protons from the BCT to the focal point of the CNGS target is also known with millimetre accuracy.

The distance between the target focal point and the OPERA reference frame was precisely measured in 2010 following a dedicated geodesy campaign. The coordinates of the origin of the OPERA reference frame were measured by establishing GPS benchmarks at the two sides of the ~10 km long Gran Sasso highway tunnel and by transporting their positions with a terrestrial traverse down to the OPERA detector. A common analysis in the ETRF2000 reference frame of the 3D coordinates of the OPERA origin and of the target focal point allowed the determination of this distance to be (730534.61 ± 0.20) m [25]. The 20 cm uncertainty is dominated by the long underground link between the outdoors GPS benchmarks and the benchmark at the OPERA detector [25].

The high-accuracy time-transfer GPS receiver allows to continuously monitor tiny movements of the Earth's crust, such as continental drift that shows up as a smooth variation of less than 1 cm/year, and the detection of slightly larger effects due to earthquakes. The April 2009 earthquake in the region of LNGS, in particular, produced a sudden displacement of about 7 cm, as seen in Fig. 7. All mentioned effects are within the accuracy of the baseline determination.
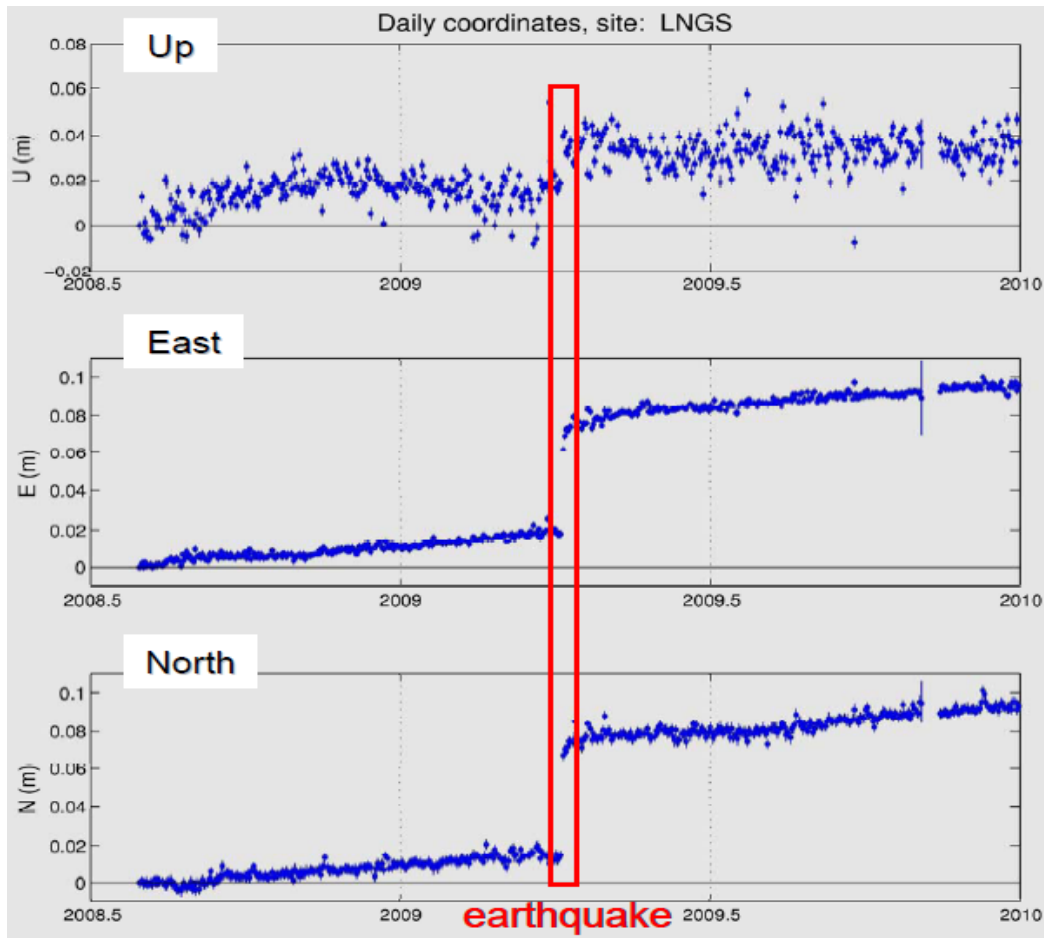

Fig. 7: Monitoring of the PolaRx2e GPS antenna position at LNGS, showing the slow earth crust drift and the fault displacement due to the 2009 earthquake in the L'Aquila region. Units for the horizontal (vertical) axis are years (metres).

Tidal effects occurring during the geodesy measurements were corrected for by expressing the results in a conventional tide-free frame [27]. Therefore, measurements taken at different times can be directly compared. As far as the neutrino baseline is concerned, periodic tidal movements are below the 1 cm level and are averaged over the long data-taking period [25].

The baseline considered for the measurement of the neutrino velocity is then the sum of (730534.61 ± 0.20) m between the CNGS target focal point and the origin of the OPERA detector reference frame, and (743.391 ± 0.002) m between the BCT and the focal point, *i.e.* (731278.0 ± 0.2) m.

5. Data selection

The OPERA data acquisition system (DAQ) time-tags the detector TT hits with 10 ns quantization with respect to the UTC [28]. The time of a neutrino interaction is defined as that of the earliest hit in the TT. CNGS events are preselected by requiring that they fall within a window of ± 20 μs with respect to the SPS kicker magnet trigger-signal, delayed by the neutrino time of flight assuming the speed of light and corrected for the various delays of the timing systems at CERN and OPERA. The relative fraction of cosmic ray events accidentally falling in this window is 10^{-4} and it is therefore negligible [1, 29].

Since TOF_c is computed with respect to the origin of the OPERA reference frame, located beneath the most upstream spectrometer magnet, the time of the earliest hit for each event is corrected for its distance along the beam line from this point, assuming time propagation at the speed of light. The UTC time of each event is also individually corrected for the instantaneous value of the time link correlating the CERN and OPERA timing systems. These corrections reflect the instability of the standard GPS systems at CERN and LNGS, whose time bases may vary by several tens of nanoseconds with respect to each other on a few hours scale.

The total statistics used for this analysis (15223 events) includes 7235 internal (charged and neutral current interactions) and 7988 external (charged current) events. Internal events, preselected by the electronic detectors with the same procedure used for neutrino oscillation studies [30], constitute a subsample of the entire OPERA statistics (about 70%) for which both time transfer systems at CERN and LNGS were operational, as well as the database-logging of the proton waveforms. As mentioned before, external events, in addition, are requested to have a muon identified in the detector.

The final statistics of 15223 neutrino interactions does not include about 5% of the preselected events, characterized by an earliest hit isolated in time and in position inside the detector with respect to the bulk of the event hits, which were discarded. Such isolated hits may be due to noise not included in the simulations and therefore constitute a potential source of bias towards early arrival times. For the retained events there is good agreement between data and simulations as far as the timing of the earliest hit is concerned. This is discussed in the next section.

6. Neutrino event timing

The schematic of the SPS/CNGS timing system is shown in Fig. 3. A general-purpose timing receiver "Control Timing Receiver" (CTRI) at CERN [31] logs every second the difference in time between the 1PPS outputs of the Xli and of the more precise PolaRx2e GPS receivers, with 0.1 ns resolution. The Xli 1PPS output represents the reference point of the time link to OPERA. This point is also the source of the "General Machine Timing" chain (GMT) serving the CERN accelerator complex [32].

The GPS devices are located in the CERN Prévessin Central Control Room (CCR). The time information is transmitted via the GMT to a remote CTRI device in Hall HCA442 (former UA2 experiment counting room) used to UTC time-stamp the kicker magnet signal. This CTRI also produces a delayed replica of the kicker magnet signal, which is sent to the adjacent WFD module. The UTC time-stamp marks the start of the digitisation window of the BCT signal. The latter signal is brought via a coaxial cable to the WFD at a distance of 100 m. Three delays characterise the CERN timing chain:

1. The propagation delay through the GMT of the time base of the CTRI module logging the PolaRx2e 1PPS output to the CTRI module used to time-tag the kicker pulse $\Delta t_{UTC} = (10085 \pm 2)$ ns;
2. The delay to produce the replica of the kicker magnet signal from the CTRI to start the digitisation of the WFD $\Delta t_{trigger} = (30 \pm 1)$ ns;
3. The delay from the time the protons cross the BCT to the time a signal arrives to the WFD $\Delta t_{BCT} = (580 \pm 5)$ ns.

The kicker signal is just used as a pre-trigger and as an arbitrary time origin. The measurement of the TOF${}_v$ is based instead on the BCT waveforms, which are tagged with respect to the UTC.

The measurement of Δt_{UTC} was performed by means of a portable Cs4000 oscillator. Its 1PPS output, stable to better than 1ns over a few hour scale, was input to the CTRI used to log the Xli 1PPs signal at the CERN CCR. The same signal was then input to the CTRI used to time-stamp the kicker signal at the HCA442 location. The two measurements allowed the determination of the delay between the time bases of the two CTRI, and to relate the kicker time-stamp to the Xli output. The measurements were repeated three times during the last two years and yielded the same results within 2 ns. This delay was also determined by performing a two-way timing measurement with optical fibres. The Cs clock and the two-way measurements also agree within 2 ns.

The two-way measurement is a technique routinely used in this analysis for the determination of delays. Measuring the delay t_A in propagating a signal to a far device consists in sending the same signal via an optical fibre B to the far device location in parallel to its direct path A. At this site the time difference t_A-t_B between the signals following the two paths is measured. A second measurement is performed by taking the signal arriving at the far location via its direct path A and sending it back to the origin with the optical fibre B. At the origin the time difference between the production and receiving time of the signal corresponds to t_A+t_B. In

this procedure the optoelectronic chain used for the fibre transmission of the two measurements is kept identical by simply swapping the receiver and the transmitter between the two locations. The two combined measurements allow determining t_A [33]. For the Δt_{UTC} the two-way setup was left in operation since July 2011 to assess the time stability of the results. The measured Δt_{UTC} showed excursions not exceeding 0.4 ns related to temperature variations of the ~ 2 km long fibres and of the associated electronics.

Measurements by two-way fibre and transportable Cs clock were systematically compared for the determination of the various delays of the CERN and OPERA timing chains and agreed within 1 ns. The two techniques are based on an inclusive measurement of the delay between pairs of reference points. This does not introduce any bias that could be related to calibration of individual hardware elements of the chain.

$\Delta t_{trigger}$ was estimated by an accurate oscilloscope measurement. The determination of Δt_{BCT} was first performed by measuring the 1PPS output of the Cs4000 oscillator with a digital oscilloscope and comparing to a CTRI signal at the point where the BCT signal arrives at the WFD. This was compared to a similar measurement where the Cs4000 1PPS signal was injected into the calibration input of the BCT. The time difference of the 1PPS signals in the two configurations led to the measurement of $\Delta t_{BCT} = (581 \pm 10)$ ns.
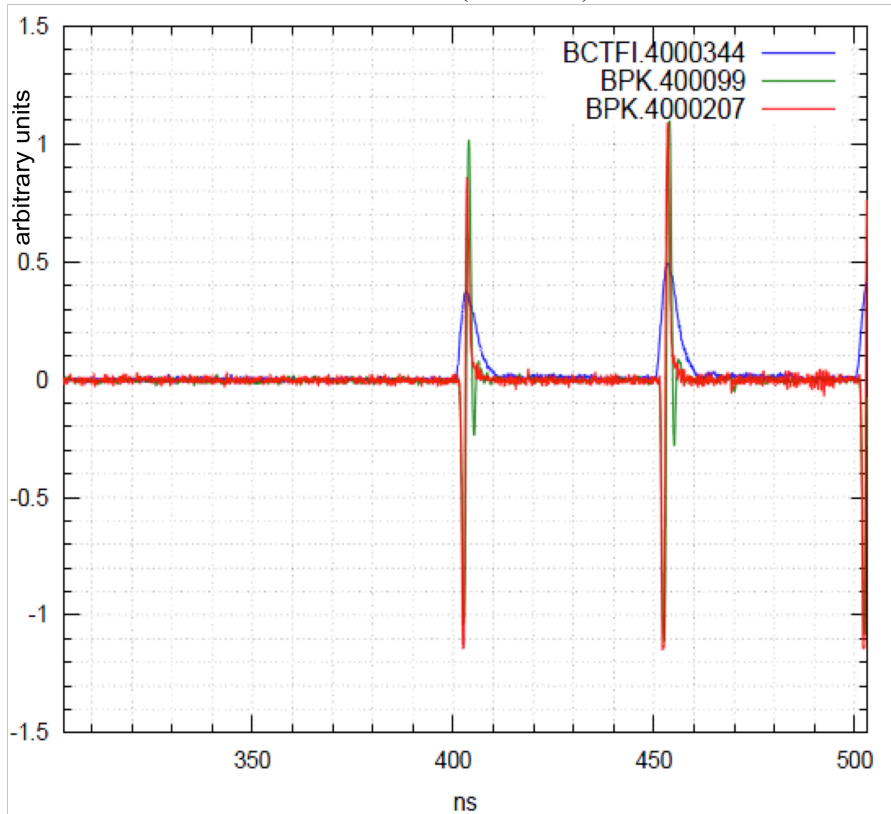

Fig. 8: Comparison between the signals of the BCT and of the fast pick-up detectors after compensating for Δt_{BCT}.

Since the above determination through the calibration input of the BCT might not be representative of the internal delay of the BCT with respect to the transit time of the protons, and also because the error on this measurement was by far the largest contribution to the overall

13

systematic uncertainty, a more sophisticated method was then applied. The proton transit time was tagged upstream of the BCT by two fast beam pick-ups BPK400099 and BPK400207 with a time response of ~1 ns [34]. From the relative positions of the three detectors (the pick-ups and the BCT) along the beam line and the signals from the two pick-ups one determines the time the protons cross the BCT and the time delay at the level of the WFD. In order to achieve an accurate determination of the delay between the BCT and the BPK signals, a measurement was performed in the particularly clean experimental condition of the SPS proton injection to the Large Hadron Collider (LHC) machine of 12 bunches with a width of about 1 ns and with 50 ns spacing, passing through the BCT and the two pick-up detectors. This measurement was performed simultaneously for the 12 bunches and yielded $\Delta t_{BCT} = (580 \pm 5 \text{ (sys.)})$ ns. The systematic error also accounts for uncertainties on the modelling of the time response of the BCT, including cables and electronics, which results in a broadening of the digitised signal with respect to the proton current pulse. This is illustrated in Fig. 8 for proton bunches of 1 ns.

Table 1: Summary of the time delay values used in the blind analysis and those corresponding to the final analysis. Only quantities that changed from the blind to the final analysis are reported

	Blind analysis (ns) 2006	Final analysis (ns) 2011	Correction (ns)
Baseline	2440079.6	2439280.9	
Earth rotation		2.2	
Correction baseline			-796.5
CNGS delays:			
UTC calibration	10092.2	10085.0	
Correction UTC			-7.2
WFD	0	30	
Correction WFD			30
BCT	0	-580	
Correction BCT			-580
OPERA Delays:			
TT response	0	59.6	
FPGA	0	-24.5	
DAQ clock	-4245.2	-4262.9	
Correction OPERA			17.4
GPS Corrections:			
Synchronisation	-353	0	
Time-link	0	-2.3	
Correction GPS			350.7
Total correction			**-985.6**

The schematic of the OPERA timing system at LNGS is shown in Fig. 6. The official UTC time source at LNGS is provided by a GPS system ESAT 2000 [35, 36] operating at the surface laboratory. The 1PPS output of the ESAT is logged with a CTRI module every second with respect to the 1PPS of the PolaRx2e, in order to establish a high-accuracy time link with CERN. Every millisecond a pulse synchronously derived from the 1PPS of the ESAT (PPmS) is transmitted to the underground laboratory via an 8.3 km long optical fibre. The delay of this transmission with respect to the ESAT 1PPS output down to the OPERA master clock output was

measured with a two-way fibre procedure in July 2006 and amounts to (40996 ± 1) ns. Measurements with a transportable Cs clock were also performed in April 2008 yielding the same result. The OPERA master clock is disciplined by a high-stability oscillator Vectron OC-050 with an Allan deviation of 2×10^{-12} at an observation time of 1 s. This oscillator keeps the local time in between two external synchronisations given by the PPmS signals coming from the external GPS. This signal is tagged with respect to the uncorrelated internal frequency of the 20 MHz OPERA master clock, thus producing a ± 25 ns time jitter.

The time base of the OPERA master clock is transmitted to the frontend cards of the TT. This delay (Δt_{clock}) was also measured with two techniques, namely by the two-way fibre method, and by transporting the Cs4000 clock to the two points. Both measurements provided the same result of (4263 ± 1) ns. The frontend card time-stamp is performed in a Field Programmable Gate Array (FPGA) by incrementing a coarse counter every 0.6 s and a fine counter with a frequency of 100 MHz. At the occurrence of a trigger the content of the two counters provides a measure of the arrival time. The fine counter is reset every 0.6 s by the arrival of the master clock signal that also increments the coarse counter. The internal delay of the FPGA processing the master clock signal to reset the fine counter was determined by a parallel measurement of trigger and clock signals with the DAQ and a digital oscilloscope. The measured delay amounts to (24.5 ± 1.0) ns. This takes into account the 10 ns quantization effect due to the clock period.

The delays in producing the Target Tracker signal including the scintillator response, the propagation of the signals in the WLS fibres, the transit time of the photomultiplier [8], and the time response of the OPERA analogue frontend readout chip (ROC) [37] were inclusively calibrated by exciting the scintillator strips at known positions by a UV picosecond laser [38]. The arrival time distribution of the photons to the photocathode and the time walk due to the discriminator threshold in the analogue frontend chip as a function of the signal pulse height were accurately determined in laboratory measurements and included in the detector simulation. The total time elapsed from the moment photons reach the photocathode, a trigger is issued by the ROC analogue frontend chip, and the trigger signal arrives at the FPGA, where it is time-stamped, was determined to be (50.2 ± 2.3) ns.

Since the time response to neutrino interactions depends on the position of the hits in the detector and on their pulse height, the average TT delay was evaluated by computing the difference between the exact interaction time and the time-stamp of the earliest hit for a sample of fully simulated neutrino interactions. Starting from the position at which photons are generated in each strip, the simulation takes into account all the effects determined in laboratory measurements including the arrival time distribution of the photons for a given production position, the time-walk of the ROC chip, and the measured delays from the photocathode to the FPGA. This TT delay has an average value of 59.6 ns with a RMS of 7.3 ns, reflecting the transverse event distribution inside the detector. The 59.6 ns represent the overall delay of the TT response down to the FPGA and they include the quoted delay of 50.2 ns. A systematic error of 3 ns was estimated due to the simulation procedure.

Several checks were performed by comparing data and simulated events as far as the earliest TT hit timing is concerned. Data and simulations agree within the above-mentioned systematic uncertainty of 3 ns for both the time differences between the earliest and all the following hits, and for the difference between the earliest hit and the average timing of muon
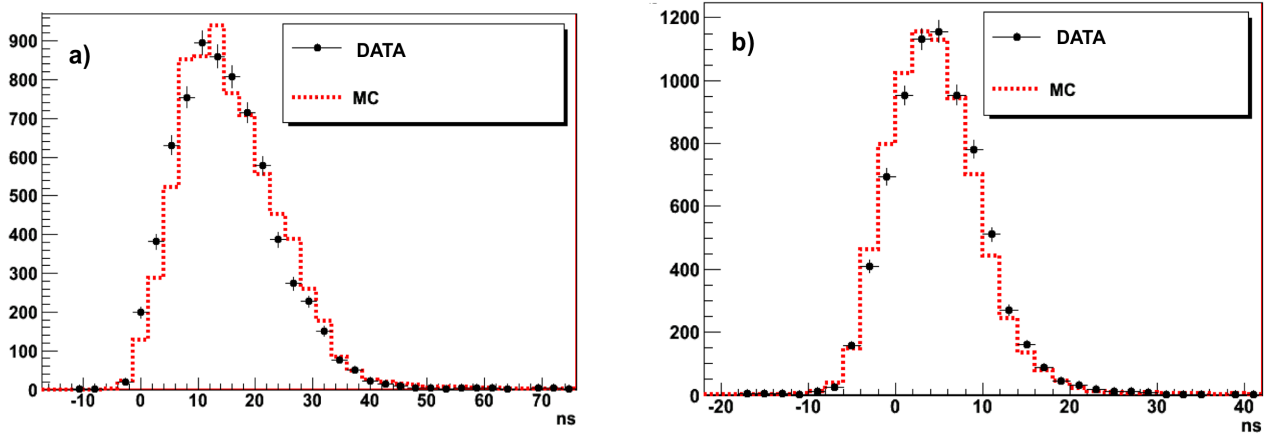
15

tracks. This is shown in Fig. 9 where the distribution of the time difference between the earliest TT hit and the average time of the event, and the average time of the muon track are shown for internal and external events, respectively. The distributions are corrected for the longitudinal position of the hits. Consequently, after correction, the truly earliest hit used to time the event may appear to be preceded by more downstream hits, hence the negative value occasionally taken by the time difference.

Fig. 9: Distribution of the time difference between the earliest TT hit and: a) the average time of the event, b) the average time of the muon track. Dots with error bars indicate data and the dotted line simulated events. Plot a) includes only internal events while plot b) only external events. The distributions are corrected for the longitudinal position of the hits.

Corrections were also applied to take into account the Sagnac effect caused by the rotation of the Earth around its axis. This yields an increase of TOF_c by 2.2 ns, with a negligible error. The Earth's revolution around the Sun and the movement of the solar system in the Milky Way induce a negligible effect, as well as the influence of the gravitational fields of Moon, Sun and Milky Way, and the Earth's frame-dragging [39]. The relative effect of the Earth's gravitational field on the Schwarzschild geodesic amounts to 10^{-8} and it is therefore totally negligible. The gravitational red-shift due to the different CERN and LNGS altitudes produces an even smaller relative effect of 10^{-13} on the clocks in between two common-view synchronisations [39].

More details on the neutrino timing and on the geodesy measurement procedures can be found in [40].

7. Data analysis

The data analysis was performed blindly by deliberately assuming the setup configuration of 2006. In particular, important calibrations were not available, such as the BCT delay Δt_{BCT}, the trigger delay $\Delta t_{trigger}$ and the improved estimate of the UTC delay Δt_{UTC}. Also TOF_c was not expressed with respect to the BCT position but referred to another conventional point upstream in the beam line. DAQ and detector delays were not taken into account either. This led by construction to an unrealistically large deviation from TOF_c, much larger than the individual

calibration contributions. The precisely calibrated corrections applied to TOF_ν and yielding the final δt value are summarised in Table 1.

For each neutrino interaction measured in the OPERA detector the analysis procedure used the corresponding proton extraction waveform. These waveforms were individually normalised to unity and summed up in order to build a PDF w(t). The white noise present at the level of individual waveforms (see the baseline of the pulses shown in Fig. 4) is averaged out by summing them up. The 200 MHz radiofrequency structure is still present in the final PDF, together with a coherent noise affecting its central part. This noise is due to an electromagnetic disturbance of the electronics in Hall HCA442, occurring with a constant delay with respect to the kicker magnet pulse. The same was observed independently by a different WFD operating in parallel and reading out another BCT detector. The noise is also present during empty spills where SPS protons are not sent to the CNGS line but to the beam dump. Since this noise is not related to the proton beam, it was filtered out by a low-pass filter applied to the final PDF. Checks were performed throughout the whole analysis chain to ensure that the filtering procedure did not affect the final results.

The WFD is triggered by the kicker magnet pulse, but the time of the proton pulses with respect to the kicker trigger is different for the two extractions. In fact, for the second extraction the kicker magnet pulse is anticipated with respect to the proton bunches, profiting of the fact that the SPS ring is half-empty. The kicker trigger is just related to the pulsing of the kicker magnet. The exact timing of the proton pulses stays within this large window of the pulse.

A separate maximum likelihood procedure was then carried out for the two proton extractions. The likelihood to be maximised for each extraction is a function of the single variable δt to be added to the time tags t_j of the OPERA events. These are expressed in the time reference of the proton waveform digitiser assuming neutrinos travelling at the speed of light, such that their distribution best coincides with the corresponding PDF:

$$L_k\left(\delta t_k\right)=\prod_j w_k\left(t_j+\delta t_k\right) \quad k = 1,2 \text{ extractions}$$

Near the maximum the likelihood function can be approximated by a Gaussian whose variance is a measure of the statistical uncertainty on δt. The data used for the maximum likelihood calculation are unbinned and the dependence on δt is computed by making a scan in steps of 1 ns. A parabolic fit is performed on the log-likelihood function for the evaluation of the maximum and of the statistical uncertainty (Fig. 10). As seen in Fig. 11, the PDF representing the time-structure of the proton extraction is not flat but exhibits a series of peaks and valleys, reflecting the features and the inefficiencies of the proton extraction from the PS to the SPS via the Continuous Transfer mechanism [41]. Such structures may well change with time. The way the PDF are built automatically accounts for the beam conditions corresponding to the neutrino interactions detected by OPERA.

The results of δt for the two proton extractions for the years 2009, 2010 and 2011 are compared in Fig. 12. They are compatible with each other. Data were also grouped in arbitrary subsamples to look for possible systematic dependences. For example, by computing δt separately for events taken during day (from 8 AM to 8 PM) and night hours, the absolute

difference between the two calculations is (16.4 ± 15.8) ns providing no indication for a systematic effect. In addition, with the presently available statistics we do not have indications of variations in the daily-24 hour observations. A similar result was obtained for a summer vs (spring plus autumn) dependence, possibly induced by thermal effects in the setup, which yielded (15.6 ± 15.0) ns. An analysis was also conducted by grouping events in two bins, corresponding to low- and high-intensity extractions (below and above 1.97×10^{13} protons on target, respectively). The absolute difference between the two bins is (6.8 ± 16.6) ns.
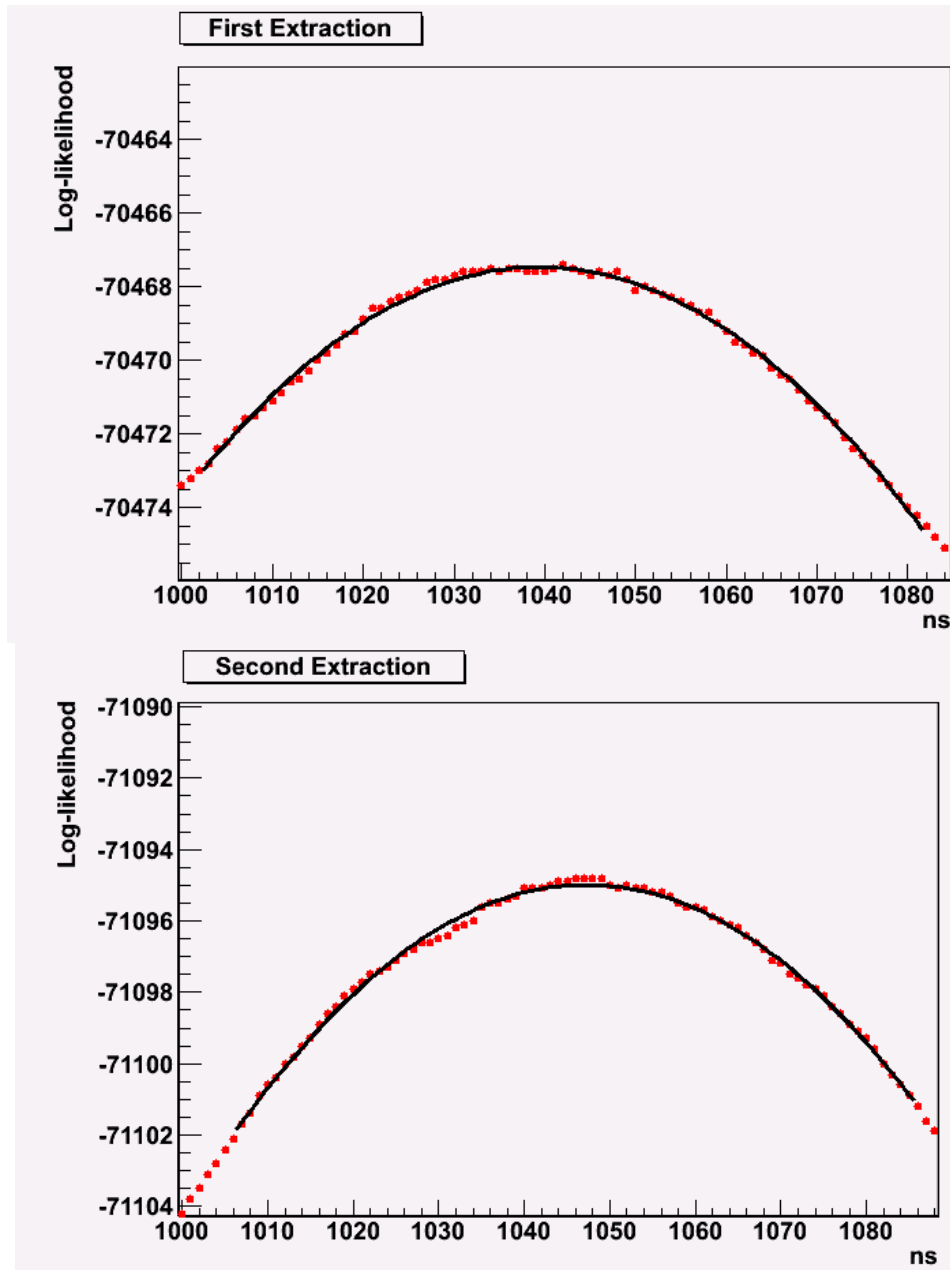
Fig. 10: Log-likelihood distributions for both extractions as a function of δt, shown close to the maximum and fitted with a parabolic shape for the determination of the central value and of its uncertainty.
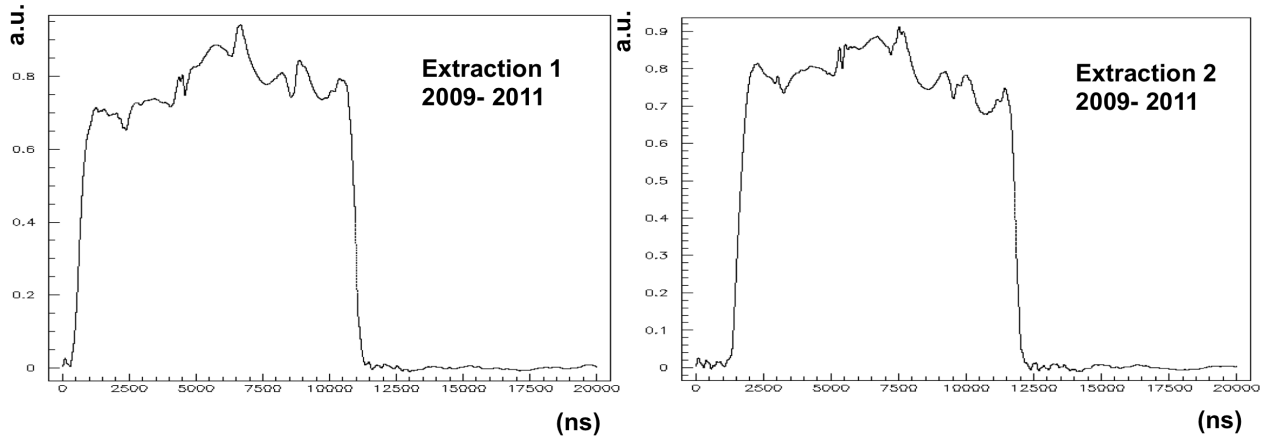
Fig. 11: Summed proton waveforms of the OPERA events corresponding to the two SPS extractions for the 2009, 2010 and 2011 data samples.
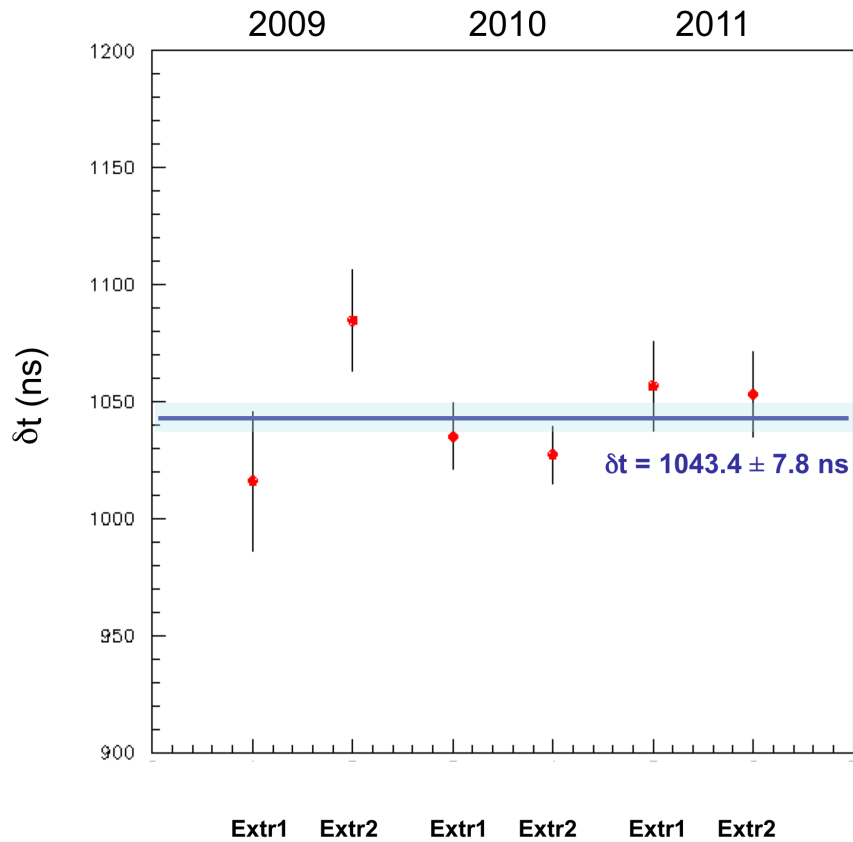

Fig. 12: Results of the maximum likelihood analysis for δt corresponding to the two SPS extractions for the 2009, 2010 and 2011 data samples.

The maximum likelihood procedure was checked with a Monte Carlo simulation. Starting from the experimental PDF, an ensemble of 100 data sets of OPERA neutrino interactions was simulated. Data were shifted in time by a constant quantity, hence faking a time of flight deviation. Each sample underwent the same maximum likelihood procedure as applied to real

19

data. The analysis yielded a result accounting for the statistical fluctuations of the sample that are reflected in the different central values and their uncertainties. The average of the central values from this ensemble of simulated OPERA experiments reproduces well the time shift applied to the simulation (at the 0.3 ns level). The average statistical error extracted from the likelihood analysis also reproduces within 1 ns the RMS distribution of the mean values with respect to the true values.
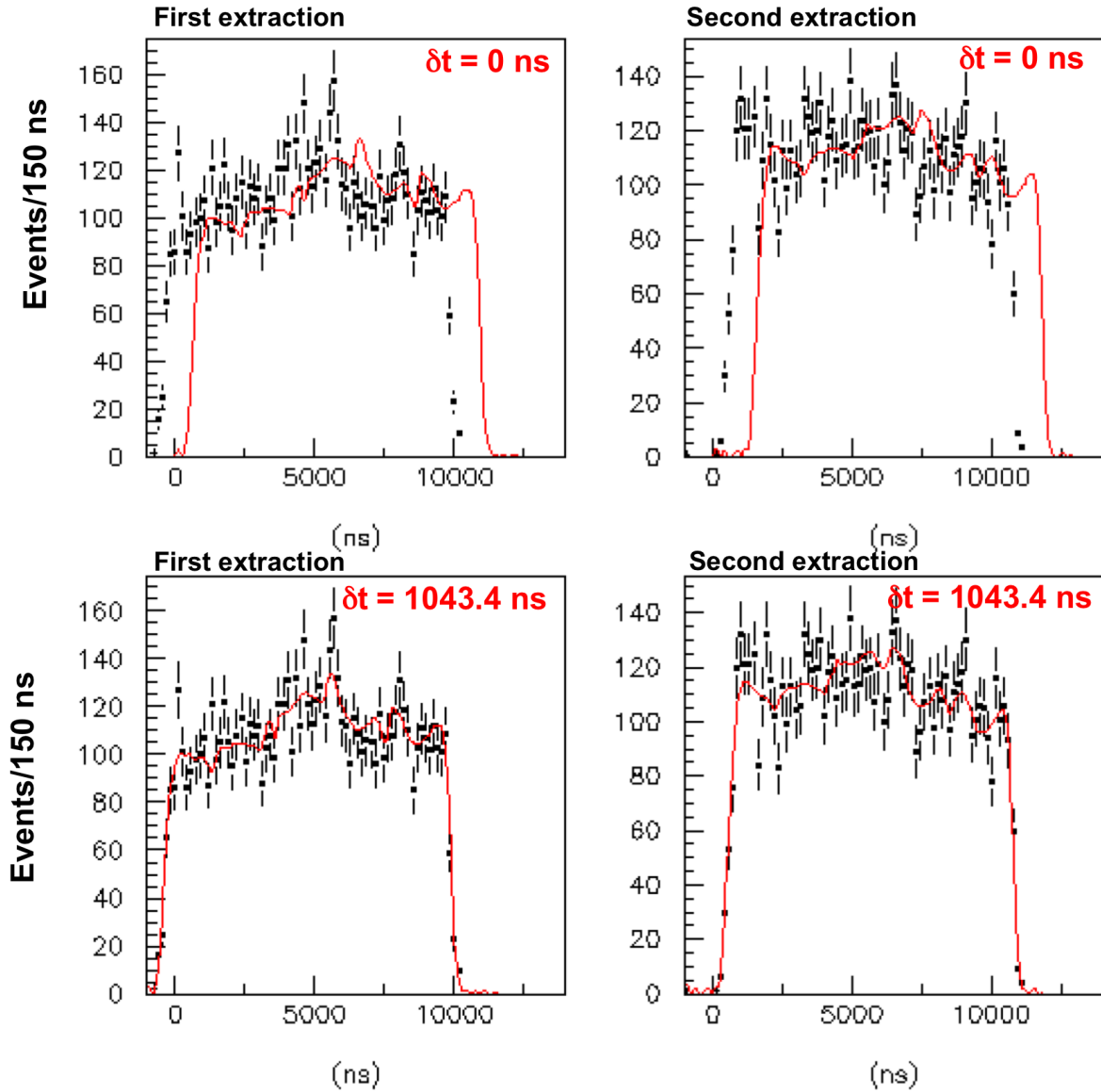

Fig. 13: Comparison of the measured neutrino interaction time distributions (data points) and the proton PDF (red line) for the two SPS extractions before (top) and after (bottom) correcting for δt (blind) resulting from the maximum likelihood analysis.
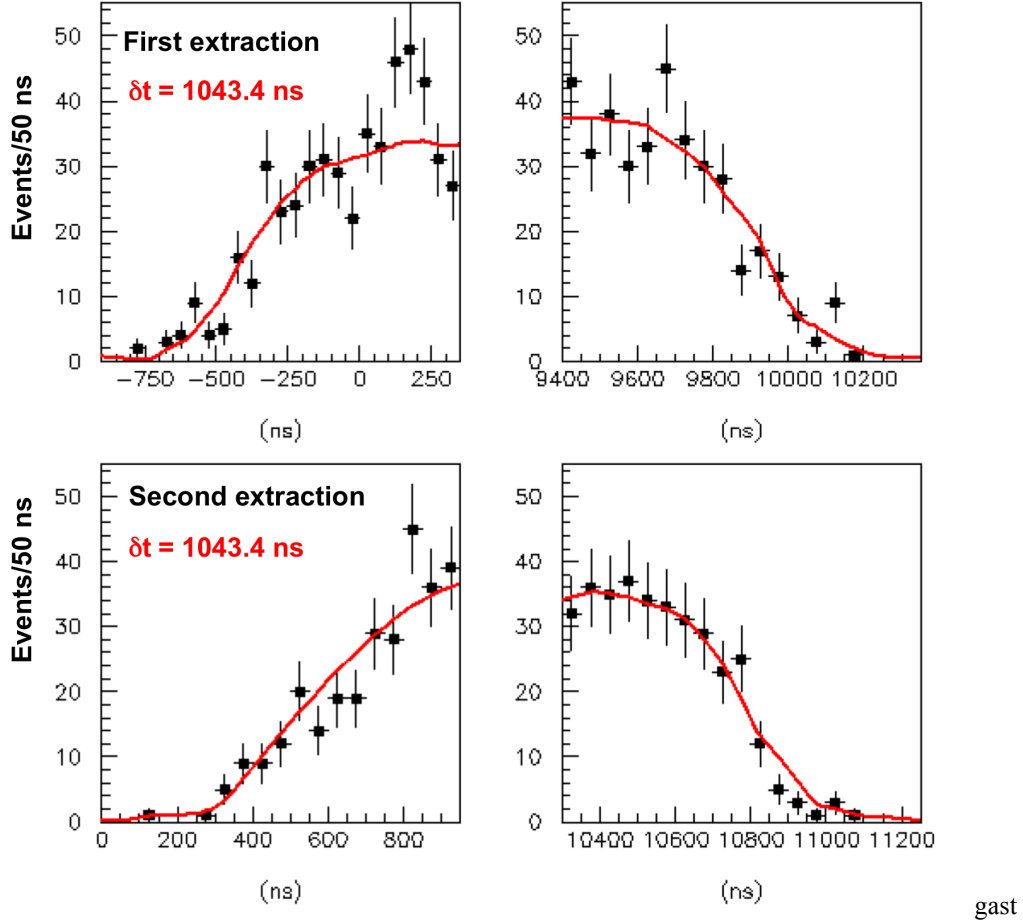
Fig. 14: Blow-up of the leading (left plots) and trailing edges (right plots) of the measured neutrino interaction time distributions (data points) and the proton PDF (red line) for the two SPS extractions after correcting for δt (blind).

The result of the blind analysis shows an earlier arrival time of the neutrinos with respect to the one computed by assuming the speed of light:

$$\delta t \text{ (blind)} = TOF_c - TOF_\nu = (1043.4 \pm 7.8 \text{ (stat.)}) \text{ ns.}$$

As a check, the same analysis was repeated considering only internal events. The result is δt (blind) = (1045.1 ± 11.3 (stat.)) ns, compatible within the systematic error of 2 ns due to the inclusion of external events. The agreement between the proton PDF and the neutrino time distribution obtained after shifting by δt (blind) is illustrated in Fig. 13. Fig. 14 shows a blow-up of the leading and trailing edges of the distributions shown at the bottom of Fig. 13. In order to perform this comparison, data were binned and shifted by the value of δt (blind) obtained from the maximum likelihood analysis. The plots in Figs. 13 and 14 only give a visual representation of the agreement between the two binned distributions, which are not used for the extraction of the value of δt.
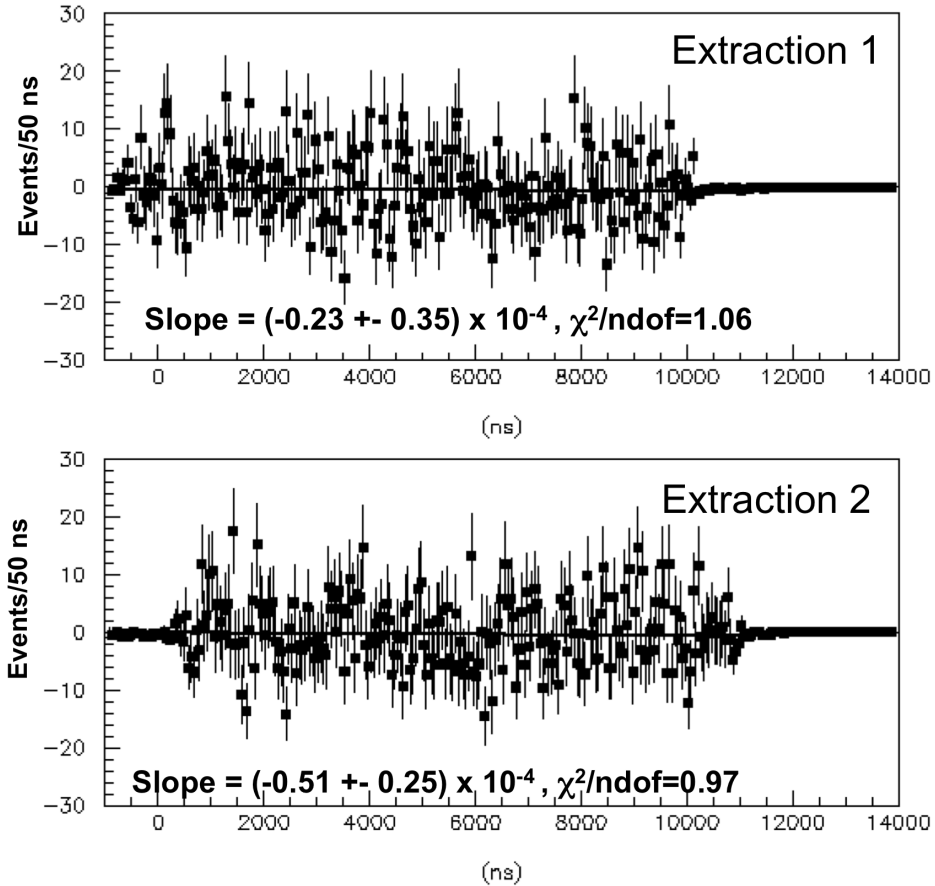
21

Fig. 15: Residuals of the data points with respect to the PDF, after correcting for δt (blind), as a function of the time since the start of the extraction. A linear fit superimposed to the experimental points gives results compatible with a flat distribution. Slopes are given in number of events per nanosecond.

The χ^2/ndf for the full distribution is 1.1 for the first extraction and 1.0 for the second one. A Kolmogorov-Smirnov test was also performed to check the agreement between the proton PDF and the neutrino event time distribution. The test gives a probability of 61.4% and 99.0%, for the first and second extraction, respectively. In addition, an Anderson-Darling test, which is more sensitive to the tails of the distributions, gives a probability of 38% and 51% for the first and second extraction, respectively.

Fig. 15 shows the residuals of the data points with respect to the PDF as a function of the time since the start of the extraction. No evidence is found for a time dependence.

Several additional statistical checks, such as the determination of δt by a χ^2 fit of the two distributions, or of parts of them separately (central region, leading and trailing edges) were performed to compare the proton PDF with the neutrino event distribution. These tests provided results comparable to those of the maximum likelihood analysis. None of them revealed any systematic effect within the present statistical accuracy, confirming the assumption that the neutrino event time distributions and the PDF are statistically equivalent.

An alternative method to extract the value of δt consists in building the likelihood function by associating each neutrino interaction to its waveform instead of using the global PDF. This method can in principle lead to smaller statistical errors given the direct comparison of each event with its related waveform. However, particular care must be taken in filtering the electronic noise, white and coherent, that affects individual waveforms, while it cancels out in the global PDF. The two extractions can be treated simultaneously in the same likelihood function defined as:

$$L\left(\delta t\right)=\prod_j w_j\left(t_j+\delta t\right)$$

Again, this procedure and the extraction of the statistical error were checked with a simulation. This method leads to a value of δt (blind) = (1040.1 ± 5.0 (stat.)) ns. A systematic error of 4.4 ns is attributed to this result by comparing different filtering conditions and treatment of the waveform baselines. This error adds up to the total systematic uncertainty whose terms are listed in Table 2 and discussed in section 8.

Finally, further investigations were conducted to search for possible systematic effects in the neutrino production mechanism by the SPS proton beam as measured by the BCT. The results are summarised below [42]:

1) The neutrino production target contains 13 graphite rods, each 10 cm long. The first 8 are interspaced by 9 cm, the last 5 by 2 mm. The diameter of the first two rods is 5 mm; the other rods have a diameter of 4 mm. The proton transfer from the BCT to the target is practically lossless. The aiming accuracy to the target centre is within 50 (90) μm RMS on the horizontal (vertical) plane. The transport of the protons to the target does not introduce any acceptance effect on the neutrino yield and on the beam profile at LNGS, which is determined by the meson decay kinematics only.

2) Density variations of the target during the time of extraction are negligible. The largest temperature increase in the graphite target corresponding to the point of maximum energy deposition (occurring around the second and the third rod) was estimated with a detailed simulation based on FLUKA and on a finite-element thermo-mechanical model of the target. This temperature increase corresponds on average to 297 K, yielding a density reduction due to transverse dilatation of 0.3%, within the 10.5 μs duration of the extraction. The total target thickness is 3.3 interaction lengths. The local density variation at the point of maximum energy deposition translates into a small displacement of this point with a negligible effect on the number of interacting protons, neutrino yield and timing distribution.

3) The current pulses of the horn and reflector magnets are 6.8 and 10 ms long, respectively; this is well above the proton extraction duration of 10.5 μs. The timing of the pulses is centred on the proton extractions and is continuously monitored. This timing is not critical with respect to the focalisation efficiency: tests were performed by artificially shifting the pulses of the magnets by as much as 100 μs. These extreme conditions produced a decrease of the muon flux associated to the neutrino beam by less than 1%, confirming the focalisation stability with respect to the pulse timing under normal operating conditions.

8. Final results

The analysis was kept blind until all geodesy measurements were performed and all the elements of the timing chains had been accurately calibrated. Corrections are summarised in Table 1. In order to ease the interpretation of the corrections a sign is attributed to each calibration value. The delays that increase (decrease) the value of $\delta t = TOF_c - TOF_\nu$ have a positive (negative) sign. In order to extract the un-blind result, each correction is computed as the difference between the value corresponding to the final analysis and the one assumed in the blind analysis.

Table 2: Contribution to the overall systematic uncertainty on the measurement of δt

Systematic uncertainties	ns	Error distribution
Baseline (20 cm)	0.67	Gaussian
Decay point	0.2	Exponential (1 side)
Interaction point	2.0	Flat (1 side)
UTC delay	2.0	Gaussian
LNGS fibres	1.0	Gaussian
DAQ clock transmission	1.0	Gaussian
FPGA calibration	1.0	Gaussian
FWD trigger delay	1.0	Gaussian
CNGS-OPERA GPS synchronisation	1.7	Gaussian
MC simulation for TT timing	3.0	Gaussian
TT time response	2.3	Gaussian
BCT calibration	5.0	Gaussian
Total systematic uncertainty	**-5.9, +8.3**	

The 17.4 ns correction in Table 1 takes into account all the effects related to DAQ and TT delays, as well as the difference between the value of Δt_{clock} determined in 2006 from a test-bench measurement and the one obtained on-site with the procedure previously described. The 353 ns relative to the 2006 calibration assume the relative synchronisation of the CERN and LNGS GPS systems prior to the installation of the two high-accuracy systems operating in common-view mode. One then obtains:

$$\delta t = TOF_c - TOF_\nu = 1043.4 \text{ ns} - 985.6 \text{ ns} = (57.8 \pm 7.8 \text{ (stat.)}) \text{ ns}.$$

This result is also affected by an overall systematic uncertainty of (-5.9, +8.3) ns coming from the combination of the different terms already discussed and summarised in Table 2. The total systematic uncertainty was computed numerically by taking into account the individual contributions and their corresponding probability distributions. The dominant uncertainty is due to the calibration of the BCT time response. The error in the CNGS-OPERA GPS synchronisation has been computed by adding in quadrature the uncertainties on the calibration performed by PTB and the internal errors of the two high-accuracy GPS systems. The final

systematic uncertainty is asymmetric. For external events, the position of the neutrino interaction in the rock is unknown and, in particular, its transverse position with respect to the detector. The distribution of the uncertainty on this position is flat. This systematically leads to an apparent increase of the neutrino time of flight TOF_ν and thus to a systematic decrease of δt.

The final result of the measurement is then:

$$\delta t = TOF_c - TOF_\nu = (57.8 \pm 7.8 \text{ (stat.) } ^{+8.3}_{-5.9} \text{ (sys.)) ns.}$$

We cannot explain the observed effect in terms of presently known systematic uncertainties. Therefore, the measurement indicates an early arrival time of CNGS muon neutrinos with respect to the one computed assuming the speed of light in vacuum. The relative difference of the muon neutrino velocity with respect to the speed of light is:

$$(v\text{-}c)/c = \delta t / (TOF'_c - \delta t) = (2.37 \pm 0.32 \text{ (stat.) } ^{+0.34}_{-0.24} \text{ (sys.)) } \times 10^{-5}.$$

If we combine statistical and systematic errors with the numerical method described above, one obtains a total uncertainty of (-9.4, +11.8) ns and a significance of 6.2 σ for rejecting the null hypothesis ($\delta t = 0$). In performing this last calculation a baseline of 730.085 km was used, and TOF'_c corresponds to this effective neutrino baseline starting from the average decay point in the CNGS tunnel as determined by simulations. Actually, the δt value is measured over the distance from the BCT to the OPERA reference frame, and it is only determined by neutrinos and not by protons and pions, which introduce negligible delays.

The alternative analysis in which the likelihood function is built by associating each neutrino interaction to its waveform instead of using the global PDF leads to a compatible value of $\delta t = (54.5 \pm 5.0 \text{ (stat.) } ^{+9.6}_{-7.2} \text{ (sys.)) ns}$. The systematic uncertainty includes the additional contribution of 4.4 ns resulting from more complex noise filtering and baseline treatment of the waveforms.

A possible neutrino energy dependence of δt was studied in order to investigate the physics origin of the early arrival time of CNGS neutrinos. For this analysis the data set was limited to ν_μ CC interactions occurring in the OPERA target (5199 events), for which the neutrino energy can be measured by adding the muon momentum to the hadronic energy. Details on the energy reconstruction in the OPERA detector are available in [15]. A first measurement was performed by using all ν_μ CC internal events. We obtained $\delta t = (61.1 \pm 13.2 \text{ (stat.) } ^{+7.3}_{-6.9} \text{ (sys.)) ns}$, for an average neutrino energy of 28.2 GeV. Data were then split into two bins of nearly equal statistics, including events of energy lower or higher than 20 GeV. The mean energies of the two samples are 13.8 and 40.7 GeV. The result for the low- and high-energy data sets are, respectively, $\delta t = (54.7 \pm 18.4 \text{ (stat.) } ^{+7.3}_{-6.9} \text{ (sys.)) ns}$ and $(68.1 \pm 19.1 \text{ (stat.) } ^{+7.3}_{-6.9} \text{ (sys.)) ns}$. The above result was checked against a full Monte Carlo simulation of the OPERA events. The same procedure used for real data was applied to ν_μ CC simulated interactions in the OPERA target. The comparison between the two data sets indicates no energy dependence. The simulation does not indicate any instrumental effects on δt possibly caused by an energy dependent time response of the detector. Therefore, the systematic uncertainties of the two measurements cancel out in

their difference, which amounts to (13.4 ± 26.5) ns. This result provides no clues about a possible energy dependence of δt in the domain explored by OPERA, within the statistical accuracy of the measurement.

9. Test with a short-bunch wide-spacing beam

In order to exclude possible systematic effects related to the use of the proton waveforms as PDF for the distributions of the neutrino arrival times within the two extractions and to their statistical treatment, a test was performed with a dedicated CNGS beam generated by a purposely setup proton beam. The modified SPS super-cycle consisted of a single extraction including four bunches about 3 ns long (FWHM) separated by 524 ns, yielding a total of ~1.1×10^{12} protons per cycle. One typical proton extraction read out by the BCT is shown in Fig. 16, while Fig. 17 shows an expanded view of an individual bunch waveform. This beam is similar to the one used for the BCT calibration discussed in section 6 and it allowed performing time of flight measurements at the single event level.
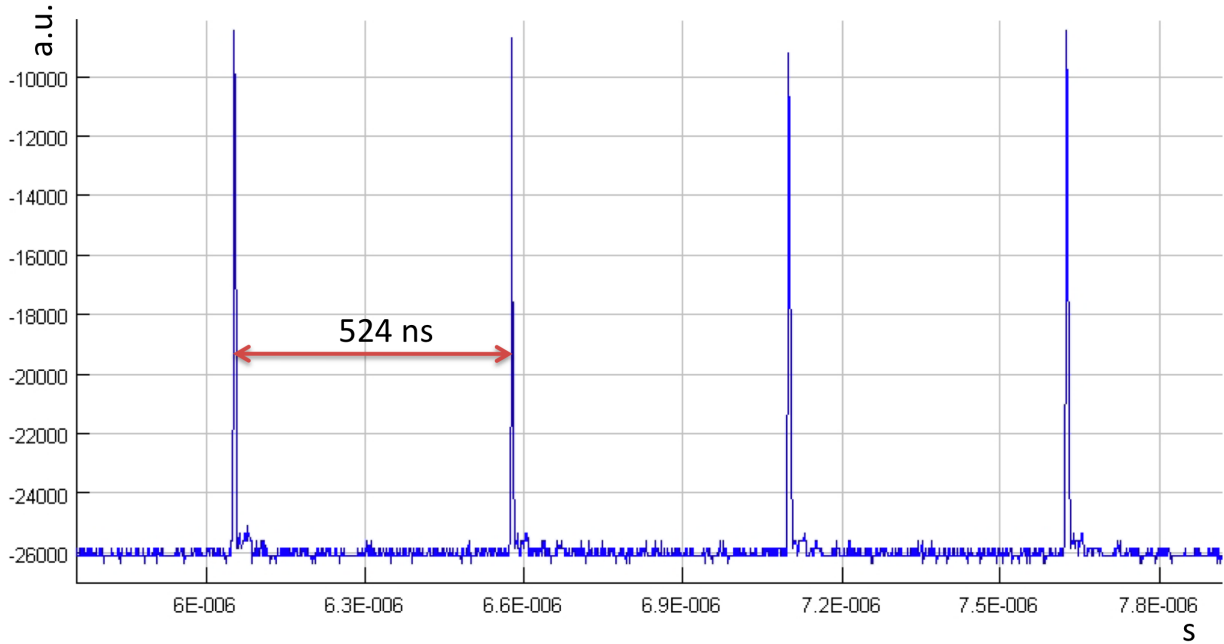
Fig. 16: Timing structure of the four-bunch proton extraction of the dedicated CNGS bunched neutrino beam as read out by the BCT detector.

Running with the CNGS bunched beam lasted from October 22 to November 6, 2011 for a total integrated intensity of 4×10^{16} protons on target. A total of 35 beam-related neutrino events were collected by OPERA. The events were then selected and reconstructed in the same way as those used for the main analysis. After selection, 6 internal and 14 external events were retained. Within the small statistics the events are evenly distributed in the four bunches of the extraction.

Given the short bunch length and the relatively long inter-bunch distance one could unambiguously associate each neutrino event to its corresponding proton bunch. The price to pay for achieving such a high definition of the neutrino emission time is the very low beam intensity, on the average about 60 times lower than for normal CNGS operation.
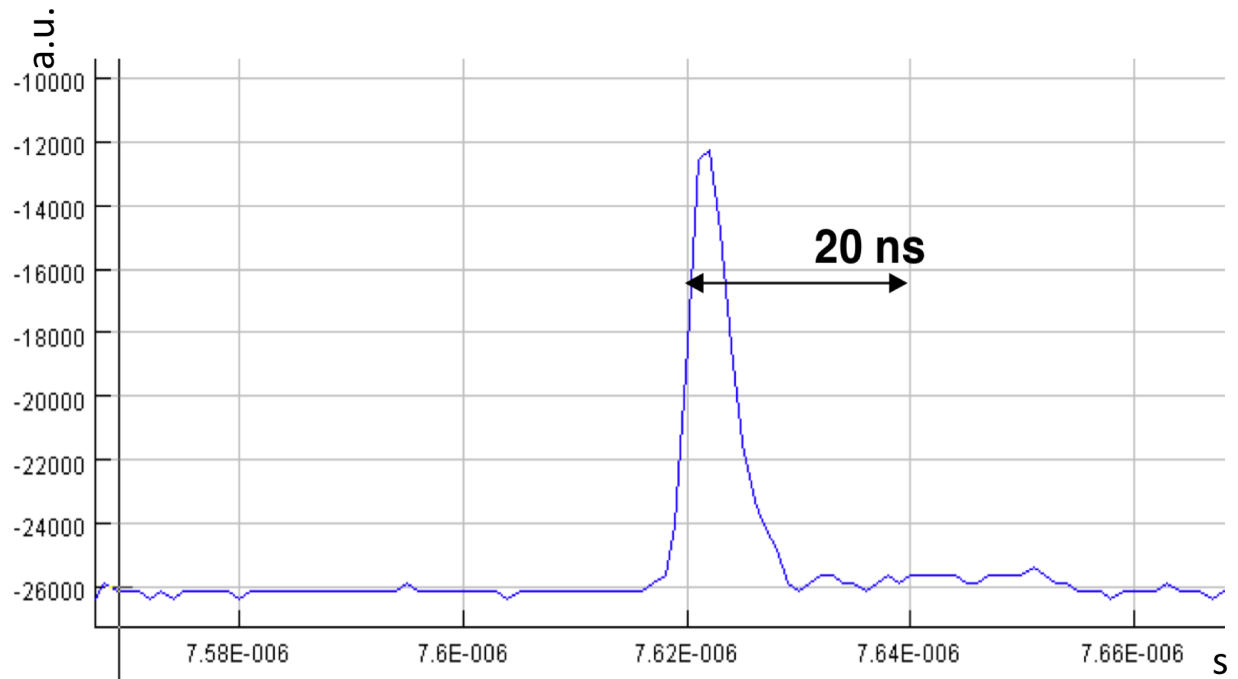
Fig. 17: Timing structure for one individual proton bunch (folded with the BCT time response).

Fig. 18 shows the distribution of the values of δt obtained for the events detected during the bunched beam test. The RMS is 16.4 ns and the average is (62.1 ± 3.7) ns in agreement with the value of (57.8 ± 7.8) ns obtained with the main analysis. At first order, systematic uncertainties related to the bunched beam operation are equal or smaller than those affecting the result with the nominal CNGS beam. The main contributions to the dispersion are given by the TT response of 7.3 ns RMS, the DAQ time granularity of 10 ns full width, and the jitter of ± 25 ns related to the tagging of the external GPS signal by the OPERA master clock. The latter dominant term results in a RMS of 14.4 ns (50 ns/√12). This dispersion is only relevant for the bunched beam measurement; nevertheless the statistical accuracy on the average δt is already as small as 3.7 ns with only 20 events.

This result largely excludes possible biases affecting the statistical analysis based on the proton PDF. It also indicates the absence of significant biases due to the cumulative response of the beam line to long proton pulses (target aiming accuracy, horns' timing, target temperature increase), as well as pulse duration effects in the BCT response. Moreover, since waveform filtering does not apply, the above considerations concern as well the procedure adopted for removing the noise.
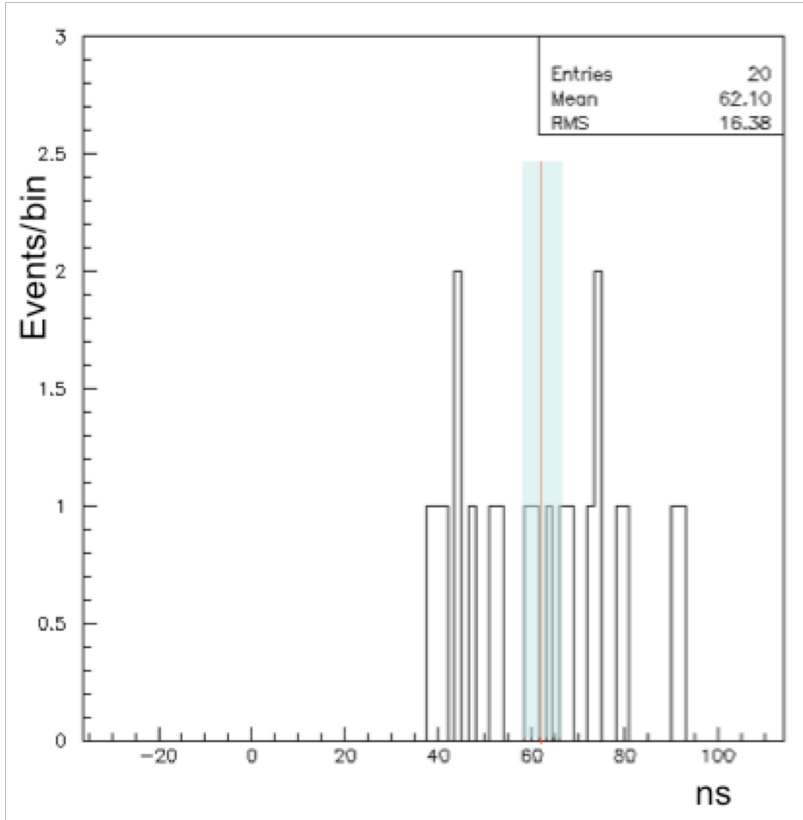
Fig. 18: Distribution of the δt values obtained from the events taken with the bunched neutrino beam. The mean value, indicated by the red line and the blue band, is (62.1 ± 3.7) ns.

10. Conclusions

The OPERA detector at LNGS, designed for the study of neutrino oscillations in appearance mode, has provided a precision measurement of the neutrino velocity over the 730 km baseline of the CNGS neutrino beam sent from CERN to LNGS through the Earth's crust. A time of flight measurement with small systematic uncertainties was made possible by a series of accurate metrology techniques. The data analysis took also advantage of a large sample of 15223 neutrino interaction events detected by OPERA.

The analysis of internal neutral current and charged current events, and external ν_μ CC interactions from the 2009, 2010 and 2011 CNGS data was carried out to measure the neutrino velocity. The sensitivity of the measurement of (v-c)/c is about one order of magnitude better than previous accelerator neutrino experiments.

The results of the study indicate for CNGS muon neutrinos with an average energy of 17 GeV an early neutrino arrival time with respect to the one computed by assuming the speed of light in vacuum:

$$\delta t = (57.8 \pm 7.8 \text{ (stat.)} \, ^{+8.3}_{-5.9} \text{ (sys.)}) \text{ ns.}$$

28

The corresponding relative difference of the muon neutrino velocity and the speed of light is:

$$(v\text{-}c)/c = (2.37 \pm 0.32 \text{ (stat.)} \, {}^{+0.34}_{-0.24} \text{ (sys.)}) \times 10^{-5},$$

with an overall significance of 6.2 σ.

An alternative analysis in which the likelihood function is built by associating each neutrino interaction to its waveform instead of using the global PDF leads to a compatible value of δt = (54.5 ± 5.0 (stat.) ${}^{+9.6}_{-7.2}$ (sys.)) ns, however affected by an additional contribution to the systematic error resulting from more complex noise filtering and baseline treatment of the waveforms.

The dependence of δt on the neutrino energy was also investigated. For this analysis the data set was limited to the 5199 ν_μ CC interactions occurring in the OPERA target. A measurement performed by considering all ν_μ CC internal events yielded δt = (61.1 ± 13.2 (stat.) ${}^{+7.3}_{-6.9}$ (sys.)) ns, for an average neutrino energy of 28.2 GeV. The sample was then split into two bins of nearly equal statistics, taking events of energy higher or lower than 20 GeV. The results for the low- and high-energy samples are, respectively, δt = (54.7 ± 18.4 (stat.) ${}^{+7.3}_{-6.9}$ (sys.)) ns and (68.1 ± 19.1 (stat.) ${}^{+7.3}_{-6.9}$ (sys.)) ns, the systematic errors cancelling out when computing their difference. This provides no clues on a possible energy dependence of δt in the domain explored by OPERA within the accuracy of the measurement.

To exclude possible systematic effects related to the use of the proton waveforms as PDF for the distributions of the neutrino arrival times within the two extractions and to their statistical treatment, a two-week long beam test was recently performed. A dedicated CNGS beam was generated by a purposely setup SPS proton beam. The modified beam consisted of a single extraction including four bunches about 3 ns long (FWHM) separated by 524 ns. With an integrated beam intensity of 4×10^{16} protons on target a total of 20 events were retained, leading to a value of δt measured from the average of the distribution of (62.1 ± 3.7) ns, in agreement with the value of (57.8 ± 7.8) ns obtained with the main analysis. At first order, systematic uncertainties related to the bunched beam operation are equal or smaller than those affecting the result obtained with the nominal CNGS beam.

In conclusion, despite the large significance of the measurement reported here and the robustness of the analysis, the potentially great impact of the result motivates the continuation of our studies in order to investigate possible still unknown systematic effects that could explain the observed anomaly. We deliberately do not attempt any theoretical or phenomenological interpretation of the results.

Acknowledgements

References

[1] OPERA Collaboration, R. Acquafredda et al., JINST 4 (2009) P04018.

[2] A. Ereditato, K. Niwa and P. Strolin, The emulsion technique for short, medium and long baseline $\nu_\mu \rightarrow \nu_\tau$ oscillation experiments, 423, INFN-AE-97-06, DAPNU-97-07;

OPERA collaboration, H. Shibuya et al., Letter of intent: the OPERA emulsion detector for a long-baseline neutrino-oscillation experiment, CERN-SPSC-97-24, LNGS-LOI-8-97;

OPERA collaboration, M. Guler et al., An appearance experiment to search for $\nu_\mu \rightarrow \nu_\tau$ oscillations in the CNGS beam: experimental proposal, CERN-SPSC-2000-028, LNGS P25/2000;

OPERA collaboration, M. Guler et al., Status Report on the OPERA experiment, CERN/SPSC 2001-025, LNGS-EXP 30/2001 add. 1/01;

OPERA Collaboration, N. Agafonova et al., Phys. Lett. B 691 (2010) 138;

OPERA Collaboration, N. Agafonova et al., arXiv:1107.2594v1.

[3] Ed. K. Elsener, The CERN Neutrino beam to Gran Sasso (Conceptual Technical Design), CERN 98-02, INFN/AE-98/05;

R. Bailey et al., The CERN Neutrino beam to Gran Sasso (NGS) (Addendum to CERN 98-02, INFN/AE-98/05), CERN-SL/99-034(DI), INFN/AE-99/05.

[4] Ch. Weinheimer et al., Phys. Lett. B 460 (1999) 219;

Ch. Weinheimer et al., Phys. Lett. B 464 (1999) 352;

M. Lobashev et al., Phys. Lett. B 460 (1999) 227.

[5] G. R. Kalbfleisch , Phys. Rev. Lett. 43, 1361 (1979);

J. Alspector et al., Phys. Rev. Lett. 36, 837 (1976).

[6] MINOS Collaboration, P. Adamson at al., Phys. Rev. D 76 (2007) 072005.

[7] K. Hirata et al., Phys. Rev. Lett. 58 (1987) 1490;

R. M. Bionta et al., Phys. Rev. Lett. 58 (1987) 1494;

M. J. Longo, Phys. Rev. D 36 (1987) 3276.

[8] Hamamatsu Photonics K.K., Electron Tube Center, 314-5, Shimokanzo, Toyooka-village, Iwata-gun, Shizuoka-ken 438–0193, Japan.

[9] T. Adam et al., Nucl. Instr. and Meth. A 577 (2007) 523.

[10] http://www.symmetricom.com/products/gps-solutions/gps-time-frequency-receivers/XLi/.

[11] H. Jacob et al., CERN-AB 2003-056 BDI.

[12] Agilent Acqiris digitiser model DP110: http://www.agilent.com -> Technical support -> Manuals -> Part number U1067A.

[13] K. Nakamura et al. (Particle Data Group), J. Phys. G 37, 075021 (2010).

[14] FLUKA software package: http://www.fluka.org; CNGS neutrino flux calculations:

http://www.mi.infn.it/~psala/Icarus/cngs.html ; G. Battistoni et al., AIP Conference Proceedings, 896m (2007) 31.

[15] OPERA Collaboration, N. Agafanova et al., New J. Phys. 13 (2011) 053051.

[16] P. Defraigne et al., Initial testing of a new GPS receiver, the PolaRx2e, for time and frequency transfer using dual frequency codes and carrier phases, in: 35th Annual Precise Time and Time Interval (PTTI) Meeting.

[17] D. W. Allan and M. A. Weiss, Accurate time and frequency transfer during common-view of a GPS satellite, in: Proc. 34th Ann. Freq. Control Symposium, USAERADCOM, Ft. Monmouth, WJ 07703, May 1980.

[18] Symmetricon frequency standards, Symmetricom, Time and Frequency System.

http://www.symmetricom.com/products/frequency-references/cesium-frequency-standard/Cs4000/.

[19] D. Allan and C. Thomas, Technical Directives for Standardization of GPS Time Receiver Software to be implemented for improving the accuracy of GPS common-view time transfer, Metrologia 31, 1994;

J. Asoubin and W. Lewandowksi, CGGTTS GPS/GLONASS Data Format V02, BIPM November 1998.

[20] P. Defraigne and G. Petit, Time Transfer to TAI Using Geodetic Receivers, Metrologia, 40, 184 (2003);

J. Levine, A review of Time and Frequency Transfer Methods, Metrologia, 45, 184 (2008).

[21] METAS Measurement Reports No 119-00210, No 119-00209: Differential calibration of matched GPS receiver, antenna and cable against reference GPS link METAS WAB2 CH01 for P3 common-view time transfer.

Physikalisch-Technische Bundesanstalt (PTB), http://www.ptb.de.

[22] T. Feldmann, "Relative calibration of the GPS time link between CERN and LNGS, Report calibration CERN-LNGS 2011", OPERA public note 134 (2011), http://operaweb.lngs.infn.it:2080/Opera/publicnotes/note134.pdf.

[23] T. Feldmann et al., Advanced GPS-based time link calibration with PTB's new GPS calibration setup, 42nd Annual Precise Time and Time Interval (PTTI) Meeting.

[24] IERS, http://www.iers.org/nn_11216/IERS/EN/IERSHome/home.html;

C. Boucher and Z. Altamimi, Memo: Specifications for reference frame fixing in the analysis of a EUREF GPS campaign, http://etrs89.ensg.ign.fr/memo-V7.pdf.

[25] G. Colosimo, M. Crespi, A. Mazzoni, F. Riguzzi, M. Jones and D. Missiaen, "Determination of the CNGS global geodesy", OPERA public note 132 (2011), http://operaweb.lngs.infn.it:2080/Opera/publicnotes/note132.pdf.

[26] EUREF Permanent Network, http://www.epncb.oma.be/.

[27] IERS Conventions 2003, http://www.iers.org/IERS/EN/Publications/TechnicalNotes/tn32.html.

[28] J. Marteau for the OPERA Collaboration, Nucl. Instr. and Meth. A 617 (2010) 291.

[29] OPERA Collaboration, R. Acquafredda, et al., New J. Phys. 8 (2006) 303.

[30] A. Bertolin and N. T. Tran, OpCarac: an algorithm for the classification of the neutrino interactions recorded by OPERA, OPERA public note 100 (2009); http://operaweb.lngs.infn.it:2080/Opera/publicnotes/note100.pdf.

[31] P. Alvarez, The CTR user guide, 17 July 2007, CERN EDMS document of the beam timing group;

J. Serrano et al., Nanosecond level UTC timing generation and stamping in the CERN's LHC, proceedings of ICALEPCS2003, 119 (2003).

[32] J. Lewis et al., The evolution of the CERN SPS timing system for the LHC era, proceedings of ICALEPCS2003, 125 (2003).

[33] J. Serrano et al., Inter-laboratory synchronisation for the CNGS project, proceedings of EPAC2006, 3092 (2006).

[34] L. Jensen, Beam Instrumentation for the CNGS facility, AB-Note-2006-022 BI.

[35] Master clock GPS 2000, http://www.esat.it/EN/default.htm, M. Ambrosio, et al., Phys. Rev. D 62 (2000) 052003.

[36] M. Ambrosio et al., The MACRO detector at Gran Sasso, Nucl. Instr. and Meth. in Physics Research A 486 (2002) 663.

[37] A. Lucotte et al., Nucl. Instr. and Meth. A 521 (2004) 378392.

[38] A. L.S. GmbH; The Picosecond Laser Diode Systems, http://www.alsgmbh.com/pilas.htm.

[39] E. Kiritsitis and F. Nitti, Special and general relativity corrections to the OPERA neutrino velocity measurement, OPERA public note 136 (2011), http://operaweb.lngs.infn.it:2080/Opera/publicnotes/note136.pdf.

[40] Neutrino velocity measurement with the OPERA experiment in the CNGS beams, G. Brunetti, PhD thesis, in joint supervision from Université Claude Bernard Lyon-I and Università di Bologna, 2011, http://operaweb.lngs.infn.it:2080/Opera/ptb/theses/theses/Brunetti-Giulia_phdthesis.pdf.

[41] C. Bovet et al., The fast shaping ejection for beam transfer from the CPS to the CERN 300 GeV machine, Proc. 1973 Particle Accelerator Conference, S. Francisco, IEEE Trans. Nucl. Sci. 20 (1973) 438;
M. Giovannozzi et al., The CERN PS multi-turn extraction based on beam splitting in stable islands of transverse phase space: Design Report, CERN-2006-011.

[42] J.-M. Cravero, E. Gschwendtner and I. Kozsar, Setting up of the CNGS horns during the yearly CNGS beam start up, EDMS Nr. 1166177, OPERA public note 137 (2011), http://operaweb.lngs.infn.it:2080/Opera/publicnotes/note137.pdf;
L. Bruno and I. Efthymiopoulos, CNGS target – explained, OPERA public note 138 (2011), http://operaweb.lngs.infn.it:2080/Opera/publicnotes/note138.pdf.